P-07-160

Oskarshamn site investigation

$^{40}Ar/^{39}Ar$ and (U-Th)/He geochronology of samples from the cored boreholes KSH03A, KSH03B, KLX01, KLX02 and the access tunnel to the Äspö Hard Rock Laboratory

Laurence Page, Pia Söderlund
Department of Geology, Lund University

Carl-Henric Wahlgren
Geological Survey of Sweden

August 2007

Svensk Kärnbränslehantering AB
Swedish Nuclear Fuel
and Waste Management Co
Box 5864
SE-102 40 Stockholm Sweden
Tel 08-459 84 00
+46 8 459 84 00
Fax 08-661 57 19
+46 8 661 57 19

ISSN 1651-4416
SKB P-07-160

Oskarshamn site investigation

$^{40}Ar/^{39}Ar$ and (U-Th)/He geochronology of samples from the cored boreholes KSH03A, KSH03B, KLX01, KLX02 and the access tunnel to the Äspö Hard Rock Laboratory

Laurence Page, Pia Söderlund
Department of Geology, Lund University

Carl-Henric Wahlgren
Geological Survey of Sweden

August 2007

Keywords: Geochronology, Thermochronology, $^{40}Ar/^{39}Ar$ dating, (U-Th)/He dating, Amphibole, Biotite, Apatite.

Abstract

The present study, aims with the help of different geochronological systems, to reconstruct the temperature-time history of the bedrock in the Oskarshamn region, from the time of crystallization of the intrusive rocks through to the time when the rocks reached higher crustal levels and were uplifted through the c 70°C isotherm. The geochronological analytical programme has involved the analysis of different minerals in different isotopic systems with different closure temperatures. In order of decreasing closure temperature, these systems are $^{40}Ar/^{39}Ar$ dating of amphibole and biotite, and (U-Th)/He dating of apatite.

This report presents the results obtained from $^{40}Ar/^{39}Ar$ and (U-Th)/He geochronology on samples obtained from boreholes and the surface in the Oskarshamn site investigation area. $^{40}Ar/^{39}Ar$ amphibole ages generally yield the time of cooling below 500°C. $^{40}Ar/^{39}Ar$ biotite ages generally represent cooling below 300°C. (U-Th)/He apatite geochronology records the time when the rocks were uplifted through the c 70–60°C isotherm.

Surface amphibole ages of 1,773 ± 13 and 1,799 ± 4 Ma indicate initial fast cooling through 500°C of the c 1,800 Ma TIB rocks followed by slower cooling through 300°C shown by c 1,620 Ma biotite ages. The $^{40}Ar/^{39}Ar$ isotopic system in biotite has been reset at c 1,510–1,470 Ma in the Oskarshamn area. The intrusions of the Götemar and Uthammar granites appears to have had major thermal effects on rocks in their immediate surrounding causing resetting of the $^{40}Ar/^{39}Ar$ isotopic system in both biotite and amphibole, yielding ages from 1,445–1,419 Ma.

(U-Th)/He apatite geochronology from the boreholes yields consistent age-depth relationships. KLX02 is the deepest borehole, reaching down to 1,700 m. The He ages decrease linearly from 300 Ma to 150 Ma down to c 1,400 m where the slope changes direction, which indicate that an abrupt change in cooling and/or uplift rate occurred. Calculations and modeling of the He ages show that the change probably occurred as late as c 100 My ago. The exhumation rate registered from the upper part of the drill core is in perfect agreement with the exhumation rate calculated from KLX01, i.e. c 13 m/Ma. The ages from the lower part of KLX02 give an exhumation rate of c 4 m/Ma. The data set from KLX02 indicate that the slightly more rapid exhumation finally stopped at c 100 Ma.

Sammanfattning

Den här studien syftar till att, genom tillämpning av olika geokronologiska system, rekonstruera den geologiska utvecklingen med avseende på de, i Oskarshamnområdet, ingående bergarternas förändring av temperatur i förhållande till tid från tiden för kristallisation av de intrusiva bergarterna till tiden då bergarterna nått högre krustal nivå och lyftes upp genom 70-gradersisotermen. Det geokronologiska analytiska programmet inkluderar analyser av olika mineral i olika isotopsystem med olika blockeringstemeperaturer. I ordning sjunkande blockeringstemperatur är dessa system $^{40}Ar/^{39}Ar$-datering av amfibol, $^{40}Ar/^{39}Ar$-datering av biotit samt (U-Th)/He-datering av apatit.

Rapporten presenterar åldersdata från nämnda metoder från borrhåls- och ytprover i Oskarshamn undersökningsområde. $^{40}Ar/^{39}Ar$ amfibol-åldrar anger generellt tiden för avkylning under 500 °C medan $^{40}Ar/^{39}Ar$ biotit-åldrar representerar avkylning under 300 °C. (U-Th)/He apatit-systemet avspeglar tiden då bergartern lyftes upp genom 70–60 °C isotermen.

Amfibolåldrarna från ytproverna, 1 773 ± 13 och 1 799 ± 4 Ma, påvisar en inledningsvis snabb avkylning genom 500 °C av de ca. 1 800 Ma TIB-bergarterna, vilket följs av en mer långsam avkylning ner till 300 °C enligt en ca. 1 620 Ma biotitålder. I de flesta delar av området har isotopsystemet för $^{40}Ar/^{39}Ar$ biotit nollställts vid 1 510–1 470 Ma. De något yngre inrusionerna i området, Götemar och Uthammar, verkar ha haft kraftig termal påverkan på bergarterna i deras absoluta närhet, vilket påvisas av nollställning av såväl $^{40}Ar/^{39}Ar$ biotit systemet som $^{40}Ar/^{39}Ar$ amfibol systemet. Analyser av dessa prover ger åldrar på 1 445–1 419 Ma.

(U-Th)/He apatitåldrar från borrhål ger konsekvent lägre åldrar med ökat djup. KLX02, det djupaste borrhålet i området, är ca. 1 700 m djupt. I detta borrhål avtar He-åldrarna linjärt från 300 Ma vid ytan ner till 150 Ma vid 1 400 m, därefter ändrar regressionslinjen för åldrarna riktning ner till botten av hålet, vilket indikerar en abrupt förändring i avkyling- och/eller upplyftningshastighet. Beräkningar och modellering av He-åldrarna indikerar att förändringen förmodligen skett så sent som för ca. 100 miljoner år sedan. Upplyftningshastigheten som beräknats på datan från den övre delen av KLX02 stämmer överens med upplyftningshastigheten som beräknats med hjälp av datan från KLX01, dvs ca. 13 m/My. Beräkningar av upplyftningshastighet med hjälp av data från den lägre delen av KLX02 ger ca. 4 m/My. Datan från KLX02 anger att den snabbare upplyftningen avtog för c 100 miljoner år sedan och att området sedan dess inte haft någon signifikant sedimentation, erosion eller upplyftning.

Contents

1 Introduction

Geochronological data is a necessity for the understanding of the cooling and uplift history of the bedrock in the Oskarshamn region, from the time of the crystallization to the time when the rocks reached higher crustal levels and were uplifted through the c 70°C isotherm. In order to try to resolve this, the study has involved different isotopic systems for different minerals with different closure temperatures.

This document reports $^{40}Ar/^{39}Ar$ and (U-Th)/He geochronology results from drill core samples from the cored boreholes KSH03A and KSH03B in the Simpevarp subarea, KLX01 and KLX02 in the Laxemar subarea, and samples from the access tunnel to the Äspö Hard Rock Laboratory (ÄHRL). The geochronological study is one of the activities performed within the site investigation at Oskarshamn. The work was carried out in accordance with activity plan AP PS 400-05-033. In Table 1-1, controlling documents for performing this activity are listed. Both activity plan and method description are SKB's internal controlling documents.

$^{40}Ar/^{39}Ar$ geochronology can be applied to different minerals with different closure temperatures. For amphibole the closure temperature is c 500°C and for biotite it is c 300°C. The (U-Th)/He method is generally sensitive to temperatures between 40 and 80°C, with a closure temperature of c 70°C for apatite.

$^{40}Ar/^{39}Ar$ dating has been performed on samples from the drill cores KLX01, KLX02 and KSH03 (Figure 1-1), and a surface sample from the immediate vicinity to the KLX02 drill-site. (U-Th)/He dating has been performed on samples from the same drill cores as well as the access tunnel to the ÄHRL. KLX01 is a c 1,078 m long, sub-vertical borehole, KLX02 is c 1,700 m long and sub-vertical, whereas KSH03A is a c 1,000 m long borehole with an inclination of c 60°. KSH03A crosses a major fault and crush zone at 162–275 m borehole length.

The results of the geochronological analyses are stored in the primary database SICADA and are traceable by the activity plan number AP PS 400-05-033. A complete list of all samples analysed in this study, including the geochronological method that was used, is presented in Table 1-2.

The report presents the data obtained from the geochronological study together with preliminary interpretations.

Table 1-1. Controlling documents for the performance of the activity.

Activity plan	Number	Version
(U-Th)/He- och $^{40}Ar/^{39}Ar$-dateringar i Simpevarpsområdet	AP PS 400-05-033	1.0
Method descriptions	**Number**	**Version**
Metodbeskrivning för åldersdatering av mineral och bergarter	SKB MD 132.002	1.0

Figure 1-1. *General overview of the Oskarshamn site investigation area, with cored and percussion boreholes shown. The cored borehole KA1755A is not shown (drilled underground from the ÄHRL).*

Table1-2. Samples analysed for geochronological dating and methods employed. The given values (secup) for the tunnel equals approximately depth.

Sample ID	Secup	Seclow	Rock type	Mineral	Method of dating
KLX01–5	5.06	5.28	Ävrö granite	Biotite	$^{40}Ar/^{39}Ar$
KLX01–1000	1,000		Ävrö granite	Biotite	$^{40}Ar/^{39}Ar$
KLX01–200	200		Ävrö granite	Apatite	(U-Th)/He
KLX01–400	400		Ävrö granite	Apatite	(U-Th)/He
KLX01–600	600		Fine-grained granite	Apatite	(U-Th)/He
KLX01–800	800		Ävrö granite	Apatite	(U-Th)/He
PSM000026			Ävrö granite	Amphibole	$^{40}Ar/^{39}Ar$
KLX02–1600	1,604.85	1,605.39	Ävrö granite	Amphibole	$^{40}Ar/^{39}Ar$
PSM000026			Ävrö granite	Biotite	$^{40}Ar/^{39}Ar$
KLX02–200	201.79	202.29	Ävrö granite	Biotite	$^{40}Ar/^{39}Ar$
KLX02–1600	1,604.85	1,605.39	Ävrö granite	Biotite	$^{40}Ar/^{39}Ar$
PSM000026			Ävrö granite	Apatite	(U-Th)/He
KLX02–200	201.79	202.29	Ävrö granite	Apatite	(U-Th)/He
KLX02–400	399.97	400.47	Ävrö granite	Apatite	(U-Th)/He
KLX02–600	601	601.5	Ävrö granite	Apatite	(U-Th)/He
KLX02–800	798.49	799	Fine-grained dioritoid	Apatite	(U-Th)/He
KLX02–1000	1,001.1	1,001.6	Ävrö granite	Apatite	(U-Th)/He
KLX02–1200	1,200.92	1,201.42	Fine-grained diorite/gabbro	Apatite	(U-Th)/He
KLX02–1400	1,399.5	1,400	Fine-grained diorite/gabbro	Apatite	(U-Th)/He
KLX02–1600	1,604.85	1,605.39	Ävrö granite	Apatite	(U-Th)/He
KLX02–1700	1,700		Granite	Apatite	(U-Th)/He
Tunnel	0		Granite	Apatite	(U-Th)/He
Tunnel	100	approx. depth	Granite	Apatite	(U-Th)/He
Tunnel	300	approx. depth	Granite	Apatite	(U-Th)/He
Tunnel	400	approx. depth	Granite	Apatite	(U-Th)/He
Tunnel	500	approx. depth	Granite	Apatite	(U-Th)/He
KSH03A–127	126.7	126.90	Quartz monzodiorite	Amphibole	$^{40}Ar/^{39}Ar$
KSH03A–127	126.7	126.90	Quartz monzodiorite	Biotite	$^{40}Ar/^{39}Ar$
KSH03B–4	3.95	4.15	Quartz monzodiorite	Biotite	$^{40}Ar/^{39}Ar$
KSH03A–300	308.12	308.32	Ävrö granite	Biotite	$^{40}Ar/^{39}Ar$
KSH03A–1000	999.6	999.90	Ävrö granite	Biotite	$^{40}Ar/^{39}Ar$
KSH03B–4	3.95	4.15	Quartz monzodiorite	Apatite	(U-Th)/He
KSH03A–127	126.7	126.90	Quartz monzodiorite	Apatite	(U-Th)/He
KSH03A–300	308.12	308.32	Ävrö granite	Apatite	(U-Th)/He
KSH03A–520	522.87	523.18	Ävrö granite	Apatite	(U-Th)/He
KSH03A–740	740.57	740.82	Ävrö granite	Apatite	(U-Th)/He
KSH03A–1000	999.6	999.90	Ävrö granite	Apatite	(U-Th)/He

2 Objective and scope

The main goal of this study is to provide geochronological constraints on the tectonothermal history of the bedrock at the Oskarshamn site by utilizing the $^{40}Ar/^{39}Ar$ and (U-Th)/He methods to constrain the cooling history of the region. Amphibole and biotite $^{40}Ar/^{39}Ar$ ages constrain the cooling of the bedrock below 500°C and 300°C, respectively. (U-Th)/He dating of apatite give information on the cooling below a much lower temperature range of 80–40°C.

Sampling from different levels along the drill cores provides a unique opportunity to constrain paleo-uplift rates and to see the effects of offsets across deformation zones.

The study is an important complement to the study of the kinematics in brittle deformation zones according to the activity plans AP PS 400-05-096, AP PS 400-06-098 and AP PS 400-07-016, and also to the kinematic analysis of ductile and brittle-ductile shear zones in the Laxemar and Simpevarp subareas /Lundberg and Sjöström 2006/. Furthermore, the obtained results are important for the understanding of the geological evolution of the Oskarshamn region.

3 Equipment

3.1 Description of equipment

The following equipment was used for sample preparation:

- Sledge hammer.
- Rock saw.
- Jaw crusher.
- Swing-mill.
- Mill tray.
- Wilfley (water shaking) table.
- Hand magnet.
- Frantz magnet separator.
- Heavy liquids (Lithium poly-tungstat (LST)).
- Gloves.
- Binocular microscope.
- Tweezers.

The geochronological analyses were carried out using the instruments and laboratories listed below:

- Hiden Hal – 3F/PIC quadrupole mass spectrometer (Free University, Amsterdam and SUERC Scotland).
- HP4500 ICPMS (Free University, Amsterdam).
- Agilent HP7500 Utrecht.
- Thermox-II (Free University, Amsterdam).
- Micromass 5400 Mass Spectrometer (Lund University; Figure 3-1).
- New Wave Research 50W CO_2 Laser (Lund University; Figure 3-2).

Figure 3-1. *Micromass 5400 Mass Spectrometer.*

Figure 3-2. *New Wave Research 50W CO_2 Laser.*

4 Execution

4.1 Preparatory work

4.1.1 Separation for $^{40}Ar/^{39}Ar$ amphibole dating

All rock samples were crushed by hand or with a jaw-crusher and subsequently milled using a swing-mill. Samples collected for $^{40}Ar/^{39}Ar$ amphibole analyses were processed into a range of grain-sizes to make sure that there was a selection of intact amphibole crystals left. The resulting mix of grain-sizes was sieved under running water in order to divide each sample into fractions of > 2 mm, 2–1 mm, 1–0.5 mm, 0.5–0.25 and < 0.25 mm. The two fractions 1–0.5 mm and 0.5–0.25 mm were in all cases regarded as most likely to contain amphibole crystals suitable for analyses. The fractions were separated into one magnetic and one non-magnetic part using a Frantz magnetic separator. The non-magnetic parts of the two fractions were examined under a binocular microscope and amphiboles were handpicked for analysis.

4.1.2 Separation for (U-Th)/He dating and $^{40}Ar/^{39}Ar$ biotite dating

Apatite is an accessory mineral in most rock types. For this study, c 0.5 kg of each rock sample was used. For mineral separation, each sample was reduced in size by a crushing procedure using a sledgehammer, a jaw-crusher and a mill tray. After these steps, each sample was placed on a Wilfley table to remove the clay size fraction. The two heaviest fractions from the Wilfley table were collected and dried. The samples were then sieved through a 250 µm and a 75 µm mesh and the middle fraction was placed into a heavy liquid (Lithium poly-tungstat (=LST), ∂=2.84 g/cm^3) to separate the apatite from lighter minerals such as feldspar and quartz. The heavy separate was placed through a Frantz magnetic separator to remove all the magnetic minerals. All mineral separation was performed at the Department of Geology, Lund University, Sweden.

Euhedral to subhedral apatite grains were handpicked. Investigation of the grains was performed under high enlargement microscope to select those with no visible inclusions. Three to four single grains were then selected for each sample and a photographic record was compiled.

Samples selected for $^{40}Ar/^{39}Ar$ biotite analyses were going through the same crushing procedure as the samples for apatite extraction. From the Wilfley table the lightest fractions (above clay fraction) were collected for biotite separation. The samples were sieved through a 500 µm mesh and from the largest fraction biotites were handpicked under a microscope.

4.2 Analytical work

4.2.2 $^{40}Ar/^{39}Ar$ geochronology

Three amphibole and eight biotite samples were irradiated together with the TCR sanidine standard (28.34 Ma recalculated following /Renne et al. 1998/) for 35 hours in the NRG-Petten HFR RODEO facility in the Netherlands. J-Values were calculated with a precision of 0.25%. The samples were run in the new $^{40}Ar/^{39}Ar$ geochronology laboratory at the University of Lund, Sweden. The lab consists of a Micromass 5400 Mass Spectrometer with a faraday and an electron multiplier. A metal extraction line which contains 2 SAES C50-ST101 Zr-Al getters and a cold finger cooled to ca –155°C by a Polycold P100 cyrogenic refrigeration unit. One or two grains of amphibole, biotite, muscovite or K-Feldspar were loaded into a copper planchette consisting of a number of 3 mm holes. Samples were step heated using a defocused 50W CO_2 laser. Sample clean up times were 5 minutes using two hot Zr-Al SAES getters and a cold

finger with a Polycold refrigeration unit. The laser was rastered over the samples to provide even-heating of all grains. The entire analytical process is automated and runs on a Macintosh running OS 10.2 with software modified specifically for this laboratory and originally developed at the Berkeley Geochronology Center by Al Deino. Time zero regressions were fitted to data collected from 10 scans over the mass range of 40 to 36. Peak heights and backgrounds were corrected for mass discrimination, isotopic decay and interfering nucleogenic Ca-, K-, and Cl-derived isotopes. Isotopic production values for the cadmium lined position in the Petten reactor are $^{36}Ar/^{37}Ar(Ca) = 0.000270$, $^{39}Ar/^{37}Ar(Ca) = 0.000699$, and $^{40}Ar/^{39}Ar(K) = 0.00183$. ^{40}Ar blanks were calculated before every new sample and after every three sample steps.^{40}Ar blanks were between $6.0^{-3}\times10^{-16}$. Blank values for masses 39-36 were all less than 7×10^{-18}. Blank values were subtracted for all incremental steps from the sample signal. We were able to produce very good incremental gas splits using a combination of increasing time at the same laser output followed by increasing laser output. Age plateaus were determined using the criteria of /Dalrymple and Lanphere 1971/ which specifies the presence of at least three contiguous incremental heating steps with statistically indistinguishable ages and constituting greater than 50% of the total ^{39}Ar released during the experiment.

4.2.3 (U-Th)/He thermochronology

(U-Th)/He thermochronology has been carried out on 25 apatite samples. All analysis were supposed to be run at the Free University (VU), Amsterdam, Netherlands but due to technical problems with the mass-spectrometers in Amsterdam some analyses where carried out at SUERC (Scottish Universities Environmental Research Centre), East Kilbride, Scotland, in collaboration with Dr. Finlay Stuart and yet others at the University of Utrecht, Netherlands by Dr. Joaquim Juez-Larré, employed at the (VU), Amsterdam, Netherlands. Table 4-1 lists where the individual samples where analysed.

Table 4-1. (U-Th)/He laboratories.

Sample ID	Depth (m)	Sample split	He analyzed at:	U-Th analyzed at:
KLX01	5	p1	Hiden Hal-3F/PIC , SUERC, Scotland	Agilent HP7500 ICPMS, Utrecht
KLX01	5	p2	Hiden Hal-3F/PIC , SUERC, Scotland	Agilent HP7500 ICPMS, Utrecht
KLX01	200	p1	Hiden Hal-3F/PIC , VU, Amsterdam	HP4500 ICPMS, VU, Amsterdam
KLX01	200	p2	Hiden Hal-3F/PIC , VU, Amsterdam	HP4500 ICPMS, VU, Amsterdam
KLX01	400	p1	Hiden Hal-3F/PIC , VU, Amsterdam	HP4500 ICPMS, VU, Amsterdam
KLX01	400	p2	Hiden Hal-3F/PIC , VU, Amsterdam	HP4500 ICPMS, VU, Amsterdam
KLX01	600	p1	Hiden Hal-3F/PIC , VU, Amsterdam	HP4500 ICPMS, VU, Amsterdam
KLX01	600	p2	Hiden Hal-3F/PIC , VU, Amsterdam	HP4500 ICPMS, VU, Amsterdam
KLX01	800	p1	Hiden Hal-3F/PIC , VU, Amsterdam	HP4500 ICPMS, VU, Amsterdam
KLX01	800	p2	Hiden Hal-3F/PIC , VU, Amsterdam	HP4500 ICPMS, VU, Amsterdam
PSM000026	0	p1	Hiden Hal-3F/PIC , SUERC, Scotland	Agilent HP7500 ICPMS, Utrecht
PSM000026	0	p2	Hiden Hal-3F/PIC , SUERC, Scotland	Agilent HP7500 ICPMS, Utrecht
KLX02	200	p1	Hiden Hal-3F/PIC , VU, Amsterdam	HP4500 ICPMS, VU, Amsterdam
KLX02	200	p2	Hiden Hal-3F/PIC , VU, Amsterdam	HP4500 ICPMS, VU, Amsterdam
KLX02	200	p3	Hiden Hal-3F/PIC , VU, Amsterdam	HP4500 ICPMS, VU, Amsterdam
KLX02	400	p1	Hiden Hal-3F/PIC , VU, Amsterdam	HP4500 ICPMS, VU, Amsterdam
KLX02	400	p2	Hiden Hal-3F/PIC , VU, Amsterdam	HP4500 ICPMS, VU, Amsterdam
KLX02	400	p3	Hiden Hal-3F/PIC , VU, Amsterdam	HP4500 ICPMS, VU, Amsterdam
KLX02	600	p1	Hiden Hal-3F/PIC , VU, Amsterdam	HP4500 ICPMS, VU, Amsterdam
KLX02	600	p2	Hiden Hal-3F/PIC , VU, Amsterdam	HP4500 ICPMS, VU, Amsterdam
KLX02	800	p1	Hiden Hal-3F/PIC , VU, Amsterdam	HP4500 ICPMS, VU, Amsterdam

Sample ID	Depth (m)	Sample split	He analyzed at:	U-Th analyzed at:
KLX02	800	p2	Hiden Hal-3F/PIC , VU, Amsterdam	HP4500 ICPMS, VU, Amsterdam
KLX02	1,000	p1	Hiden Hal-3F/PIC , VU, Amsterdam	HP4500 ICPMS, VU, Amsterdam
KLX02	1,000	p2	Hiden Hal-3F/PIC , VU, Amsterdam	HP4500 ICPMS, VU, Amsterdam
KLX02	1,000	p3	Hiden Hal-3F/PIC , VU, Amsterdam	HP4500 ICPMS, VU, Amsterdam
KLX02	1,000	p4	Hiden Hal-3F/PIC , VU, Amsterdam	HP4500 ICPMS, VU, Amsterdam
KLX02	1,200	p1	Hiden Hal-3F/PIC , VU, Amsterdam	HP4500 ICPMS, VU, Amsterdam
KLX02	1,200	p2	Hiden Hal-3F/PIC , VU, Amsterdam	HP4500 ICPMS, VU, Amsterdam
KLX02	1,400	p1	Hiden Hal-3F/PIC , VU, Amsterdam	HP4500 ICPMS, VU, Amsterdam
KLX02	1,600	p1	Hiden Hal-3F/PIC , VU, Amsterdam	HP4500 ICPMS, VU, Amsterdam
KLX02	1,600	p2	Hiden Hal-3F/PIC , VU, Amsterdam	HP4500 ICPMS, VU, Amsterdam
KLX02	1,700	p2	Hiden Hal-3F/PIC , VU, Amsterdam	HP4500 ICPMS, VU, Amsterdam
KLX02	1,700	p3	Hiden Hal-3F/PIC , VU, Amsterdam	HP4500 ICPMS, VU, Amsterdam
Tunnel	0	p1	Hiden Hal-3F/PIC , VU, Amsterdam	HP4500 ICPMS, VU, Amsterdam
Tunnel	0	p2	Hiden Hal-3F/PIC , VU, Amsterdam	HP4500 ICPMS, VU, Amsterdam
Tunnel	100	p1	Hiden Hal-3F/PIC , VU, Amsterdam	HP4500 ICPMS, VU, Amsterdam
Tunnel	100	p2	Hiden Hal-3F/PIC , VU, Amsterdam	HP4500 ICPMS, VU, Amsterdam
Tunnel	100	p3	Hiden Hal-3F/PIC , VU, Amsterdam	HP4500 ICPMS, VU, Amsterdam
Tunnel	300	p1	Hiden Hal-3F/PIC , VU, Amsterdam	HP4500 ICPMS, VU, Amsterdam
Tunnel	300	p2	Hiden Hal-3F/PIC , VU, Amsterdam	HP4500 ICPMS, VU, Amsterdam
Tunnel	300	p3	Hiden Hal-3F/PIC , VU, Amsterdam	HP4500 ICPMS, VU, Amsterdam
Tunnel	400	p1	Hiden Hal-3F/PIC , VU, Amsterdam	HP4500 ICPMS, VU, Amsterdam
Tunnel	400	p2	Hiden Hal-3F/PIC , VU, Amsterdam	HP4500 ICPMS, VU, Amsterdam
Tunnel	500	p1	Hiden Hal-3F/PIC , VU, Amsterdam	HP4500 ICPMS, VU, Amsterdam
Tunnel	500	p2	Hiden Hal-3F/PIC , VU, Amsterdam	HP4500 ICPMS, VU, Amsterdam
KSH03B	4	p1	Hiden Hal-3F/PIC , SUERC, Scotland	Agilent HP7500 ICPMS, Utrecht
KSH03B	4	p2	Hiden Hal-3F/PIC , SUERC, Scotland	Agilent HP7500 ICPMS, Utrecht
KSH03B	4	p3	Hiden Hal-3F/PIC , SUERC, Scotland	Thermo X-II ICPMS, VU, Amsterdam
KSH03B	4	p4	Hiden Hal-3F/PIC , SUERC, Scotland	Thermo X-II ICPMS, VU, Amsterdam
KSH03A	127	p1	Hiden Hal-3F/PIC , SUERC, Scotland	Agilent HP7500 ICPMS, Utrecht
KSH03A	127	p2	Hiden Hal-3F/PIC , SUERC, Scotland	Agilent HP7500 ICPMS, Utrecht
KSH03A	127	p3	Hiden Hal-3F/PIC , SUERC, Scotland	Thermo X-II ICPMS, VU, Amsterdam
KSH03A	127	p4	Hiden Hal-3F/PIC , SUERC, Scotland	Thermo X-II ICPMS, VU, Amsterdam
KSH03A	300	p1	Hiden Hal-3F/PIC , SUERC, Scotland	Agilent HP7500 ICPMS, Utrecht
KSH03A	300	p2	Hiden Hal-3F/PIC , SUERC, Scotland	Agilent HP7500 ICPMS, Utrecht
KSH03A	300	p3	Hiden Hal-3F/PIC , SUERC, Scotland	Thermo X-II ICPMS, VU, Amsterdam
KSH03A	300	p4	Hiden Hal-3F/PIC , SUERC, Scotland	Thermo X-II ICPMS, VU, Amsterdam
KSH03A	520	p1	Hiden Hal-3F/PIC , SUERC, Scotland	Thermo X-II ICPMS, VU, Amsterdam
KSH03A	520	p2	Hiden Hal-3F/PIC , SUERC, Scotland	Thermo X-II ICPMS, VU, Amsterdam
KSH03A	740	p1	Hiden Hal-3F/PIC , SUERC, Scotland	Thermo X-II ICPMS, VU, Amsterdam
KSH03A	740	p2	Hiden Hal-3F/PIC , SUERC, Scotland	Thermo X-II ICPMS, VU, Amsterdam
KSH03A	740	p3	Hiden Hal-3F/PIC , SUERC, Scotland	Thermo X-II ICPMS, VU, Amsterdam
KSH03A	1,000	p1	Hiden Hal-3F/PIC , SUERC, Scotland	Agilent HP7500 ICPMS, Utrecht
KSH03A	1,000	p2	Hiden Hal-3F/PIC , SUERC, Scotland	Agilent HP7500 ICPMS, Utrecht
KSH03A	1,000	p3	Hiden Hal-3F/PIC , SUERC, Scotland	Thermo X-II ICPMS, VU, Amsterdam
KSH03A	1,000	p4	Hiden Hal-3F/PIC , SUERC, Scotland	Thermo X-II ICPMS, VU, Amsterdam

Helium extraction (VU, Amsterdam)

Helium measurements were conducted on a Hiden Hal-3F/PIC quadrupole mass spectrometer. For each individual sample, the single apatite grain is inserted in an inconel capsule and loaded into separate inconel tubes. The inconel tubes are mounted in a flange multiplexer and pumped to UHV-conditions (~10^{-9} mbar). Each inconel tube containing a sample was heated in an external oven up to 950°C for 30 minutes. These T-t conditions guarantee the complete extraction of helium from the apatite grain size used in this study. After each degassing and before the helium-4 is measured, a sequential clean-up procedure is carried out, consisting of: a) exposure to a SAES getter at 450°C and a SAES 707 getter for the removal of reactive gases and H_2 respectively, b) exposure to one charcoal trap held at nitrogen temperatures to isolate non-reactive condensable gases. The remaining gases (mostly helium) are then expanded into the mass spectrometer for analysis. The amount of helium is determined by peak comparison with a standard (Durango) measured under the same conditions as the samples. All samples analyzed are corrected for background levels by subtracting the hot blank signal.

Helium extraction (SUERC, Scotland)

Helium measurements were conducted on a quadruple mass spectrometer (Hiden Hal-3F/PIC). For each individual sample, the single apatite grain is inserted in platinum foil and loaded in 1.5 mm deep × 2 mm diameter holes in a 6 cm diameter high-purity Cu planchet that sits in a 11.5 cm diameter stainless steel chamber. The laser chamber is connected to the gas cleanup and analysis system, which is pumped to UHV-conditions. The primary power supply is a 25 W continuous wave fiber-coupled diode laser (FDL25: Laservall S.p.A. Donnas (Aoste), Italy) emitting at a wavelength of 808 nm. Laser radiation is generated by optical pumping in a diode laser cell, housed in a 54 × 45 × 18 cm metal enclosure. Laser power output is linearly correlated with input power at least up to 12.5 W. A 5 mW, 632 nm red He-Ne laser runs in the core and the outer 100 mm of the fiber and is used for focusing the 808 nm beam. The temperature of the Pt foils are not measured directly during heating, but are assessed by visual observation of the color emitted from heated Pt tubes. Complete degassing of apatite fragments and crystals requires heating for 30 s at 500–600°C (0.5W, using the defocused beam). Reheating the sample under the same conditions should not releases any additional He above blank levels. Gases liberated by heating the Pt-foil capsules are purified using a hot SAES TiZr getter and two liquid nitrogen cooled charcoal traps. 4He abundances along with 3He, H (mass 2) and CH4 (mass 16), are determined by an electron multiplier in a Hiden HAL3F quadrupole mass spectrometer operated in static mode. Absolute He concentrations are calculated from peak height comparison against a calibrated standard (Durango).

U-Th measurements (HP4500, VU, Amsterdam)

The grains were unloaded from the inconel capsules and the apatite was transferred to a Teflon beaker. Grains were dissolved with HNO_3 and HF on hot plates, spiked with two artificial isotopes (^{233}U and ^{229}Th) and diluted up to ~ 3 ml with MiliQwater. In this solution, the uranium and thorium contents were measured using an Inductively Coupled Plasma Mass Spectrometer (ICP-MS). The argon ICP used is a high temperature plasma fireball, into which the aerosol sample is carried by argon gas. A low-flow Teflon nebulizer (90–120 µl/min) was used in order to increase the ICP-MS efficiency for measurements of very low U-Th concentrations in small quantities of the solution. The plasma decomposes and dissociates the particles of the sample and then ionises the resulting atoms. The ions are partially extracted into the vacuum chamber, focused and transferred to a quadruple mass spectrometer, where they are analysed by an electron multiplier detector in a rapid sequential scan. Detection limits are typically at the ng/l (ppt) level. The resulting mass spectra are used to quantify the amount of ^{238}U and ^{232}Th by isotopic ratio comparison to the two artificial isotopes of known concentration.

U-Th measurements (Agilent HP7500, Utrecht and Thermo X-II, VU, Amsterdam)

Pt foils containing the apatite grains were unloaded from the Cu planchet and transferred to a 7-ml Teflon beaker. Grains are first spiked with two artificial isotopes (^{233}U and ^{229}Th) and dissolved with concentrated HNO_3 and HF on a hot plate (120°C), which will not dissolve the Pt foil. The concentrated acid is let to evaporate and samples are re-dissolved in a 0.6 ml 2 normal HNO_3 solution. Finally all solutions are diluted up to 2 ml with MiliQwater and make ready for analysis. Uranium and thorium contents were measured using a Thermo X-II ICP-MS. A low-flow Teflon nebulizer (100 µl/min) was used in order to increase the ICP-MS efficiency for measurements of very low U-Th concentrations in small quantities of the solution. The ratios between the artificial isotopes (^{233}U and ^{229}Th) and natural (^{238}U and ^{232}Th) are used to determine the concentration of the latest.

Durango standard calibration

Verification of the analytical technique and procedures is provided by routine analyses of an apatite standard. As a standard we used the 160–180 m fraction of crushed and sieved Durango apatite crystals that were originally 1–2 cm in size. Each standard aliquot analyzed contained less than 10 µg of Durango. Nine Durango standards were measured for (U-Th)/He in the analyses. The results yielded a range of (U-Th)/He ages between 31 ± 3 Ma and 34 ± 3 Ma against a reported age of 32 ± 1 Ma /McDowell et al. 2005/.

4.3 Data Handling

^{40}Ar/^{39}Ar geochronology data was produced, plotted and fitted using the argon program provided by Al Deino of the Berkeley Geochronology Centre. Data was subsequently exported to MS Excel tables. (U-Th)/He ages were calculated with an in-house program used at Vrije University, Amsterdam. Data was subsequently exported to MS Excel tables.

5 Results

The data from the geochronological study are presented in the following sections with data tables placed at the end of the relevant section: Table 5-1 $^{40}Ar/^{39}Ar$ amphibole and Table 5-2 $^{40}Ar/^{39}Ar$ biotite are placed at the end of section 5.1. Table 5-3 (U-Th)/He is presented in the beginning of section 5.2. The data are also presented in plots as appropriate for the different techniques. Step-heating spectra for the $^{40}Ar/^{39}Ar$ data are given for each sample and the $^{40}Ar/^{39}Ar$ and (U-Th)/He data are also plotted in age vs depth diagrams.

5.1 $^{40}Ar/^{39}Ar$ dating

KLX01

KLX01-5

The $^{40}Ar/^{39}Ar$ age for biotite from Ävrö granite that was sampled in the interval 5.06–5.28 m (borehole length) can be seen in Figure 5-1. The plateau age, 1,486 ± 3 Ma, is interpreted as dating the cooling below the closure temperature of biotite (c 300°C).

KLX01-1000

The $^{40}Ar/^{39}Ar$ age for biotite from Ävrö granite that was sampled at 1,000 m borehole length can be seen in Figure 5-2. The plateau age, 1,481 ± 3 Ma, is interpreted as dating the cooling below the closure temperature of biotite (c 300°C).

The $^{40}Ar/^{39}Ar$ age versus depth profile for KLX01 is provided below in Figure 5-3 and is discussed further in the conclusions section.

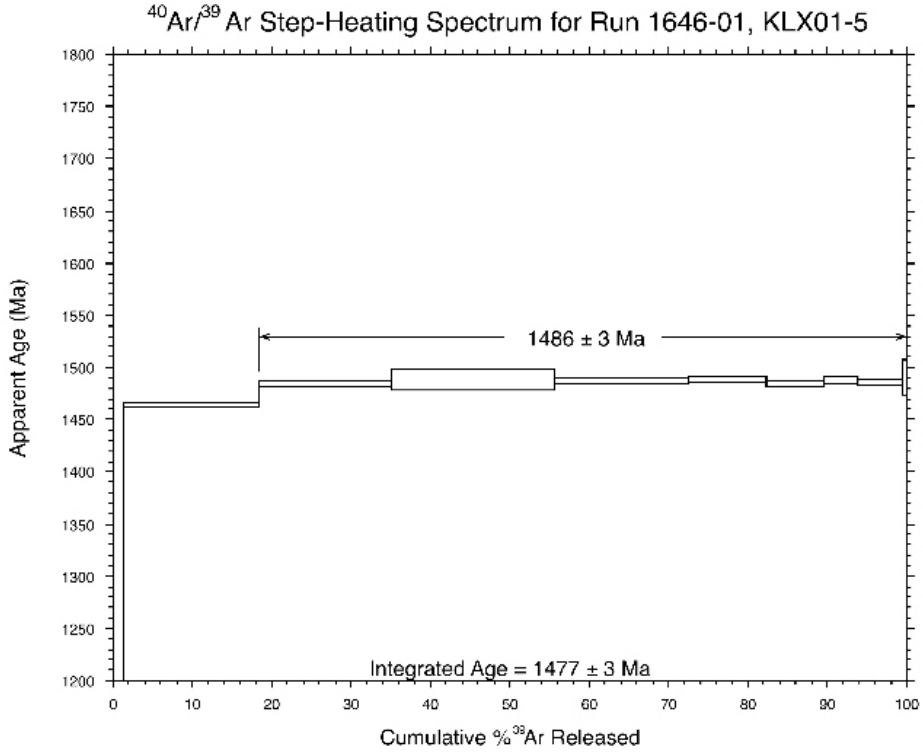

Figure 5-1. *$^{40}Ar/^{39}Ar$ biotite step-heating spectrum for sample KLX01-5.*

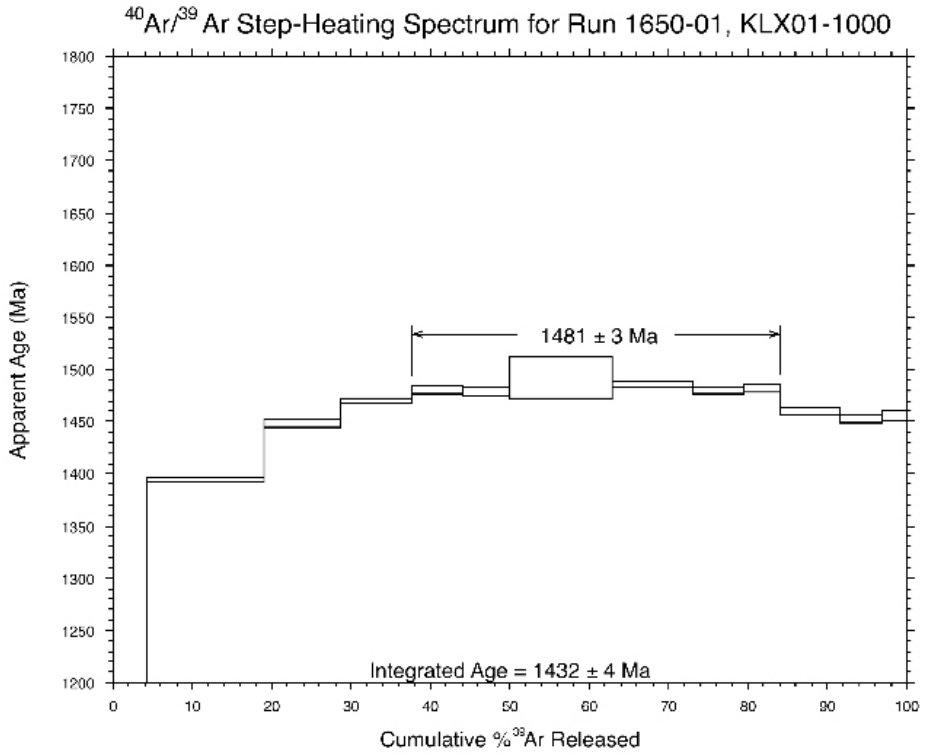

Figure 5-2. *$^{40}Ar/^{39}Ar$ biotite step-heating spectrum for sample KLX01-1000.*

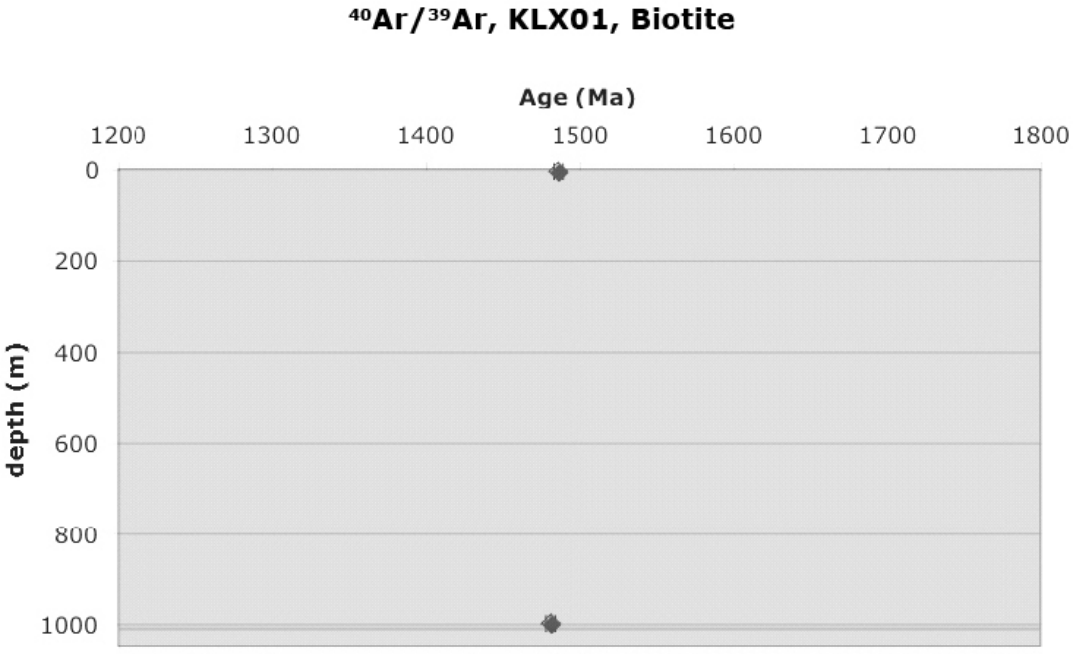

Figure 5-3. *$^{40}Ar/^{39}Ar$ biotite age vs depth profile from KLX01. The red line marks an identified deformation zone from the geological single-hole interpretation. Note that depth in the diagram corresponds to borehole length.*

KLX02 and nearby surface sample

PSM000026

The $^{40}Ar/^{39}Ar$ age for amphibole from a surface sample of the Ävrö granite can be seen in Figure 5-4. The forced plateau age, 1,773 ± 13 Ma, is interpreted as dating the cooling below the closure temperature of amphibole (c 500°C).

KLX02-1600

The,$^{40}Ar/^{39}Ar$ age for amphibole from Ävrö granite that was sampled in the interval 1,604.85–1,605.39 m (borehole length) can be seen in Figure 5-5. The forced plateau age, 1,445 ± 14 Ma, is interpreted as dating the cooling below the closure temperature of amphibole (c 500°C).

PSM000026

The $^{40}Ar/^{39}Ar$ age for biotite from a surface sample of Ävrö granite can be seen in Figure 5-6. The plateau age, 1,468 ± 2 Ma, is interpreted as dating the cooling below the closure temperature of biotite (c 300°C).

KLX02-200

Two splits of biotite from Ävrö granite that was sampled in the interval 201.79–202.29 m (borehole length) were analysed. A $^{40}Ar/^{39}Ar$ plateau age of 1,491 ± 6 Ma (Figure 5-7) and a forced fit age of 1,508 ± 7 Ma (Figure 5-8) were obtained. These ages are interpreted as dating the cooling below the closure temperature of biotite (c 300°C).

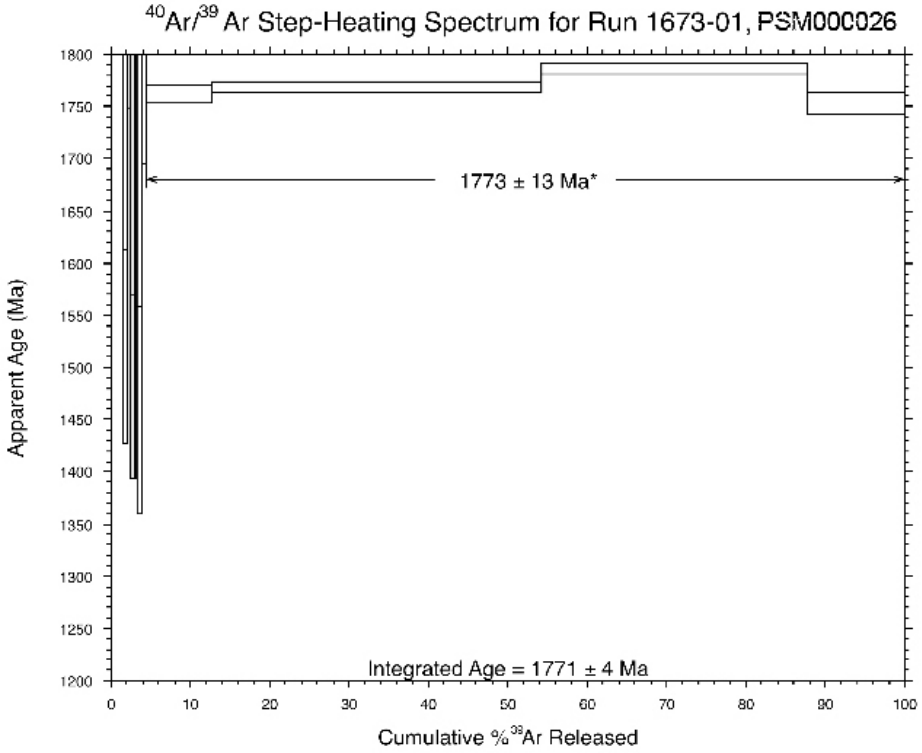

Figure 5-4. *$^{40}Ar/^{39}Ar$ amphibole step-heating spectrum for sample PSM000026.*

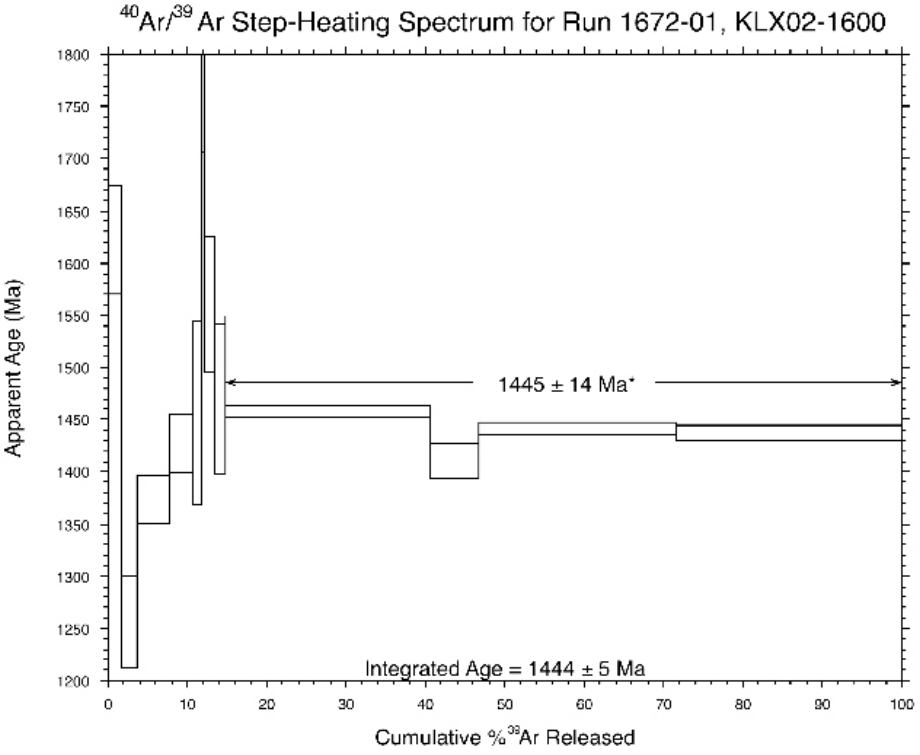

Figure 5-5. *$^{40}Ar/^{39}Ar$ amphibole step-heating spectrum for sample KLX02-1600.*

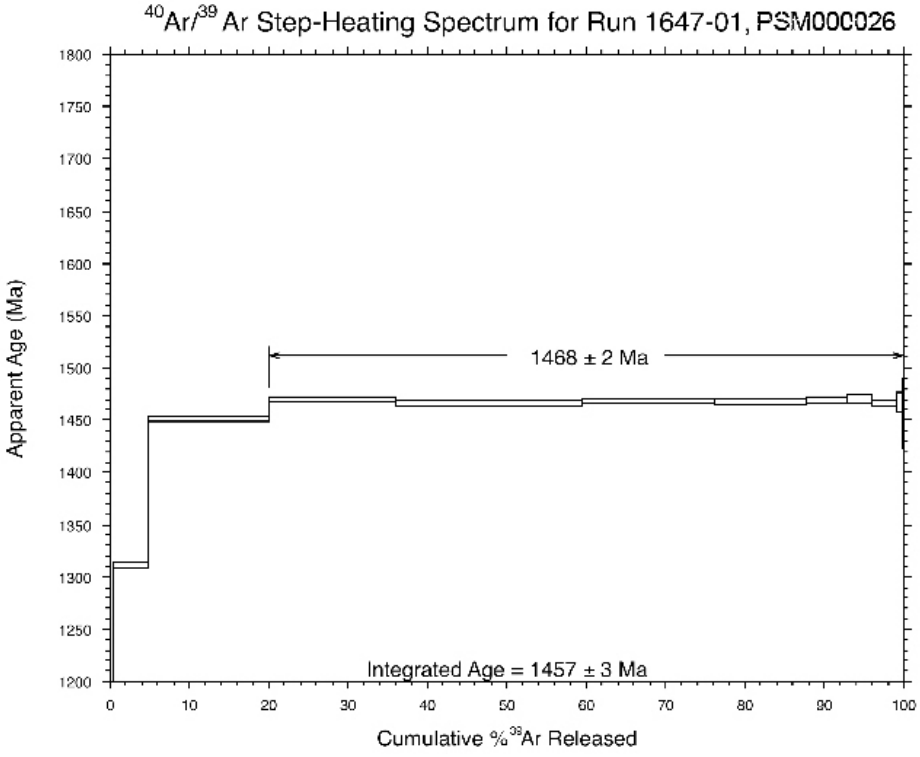

Figure 5-6. *$^{40}Ar/^{39}Ar$ biotite step-heating spectrum for sample PSM000026.*

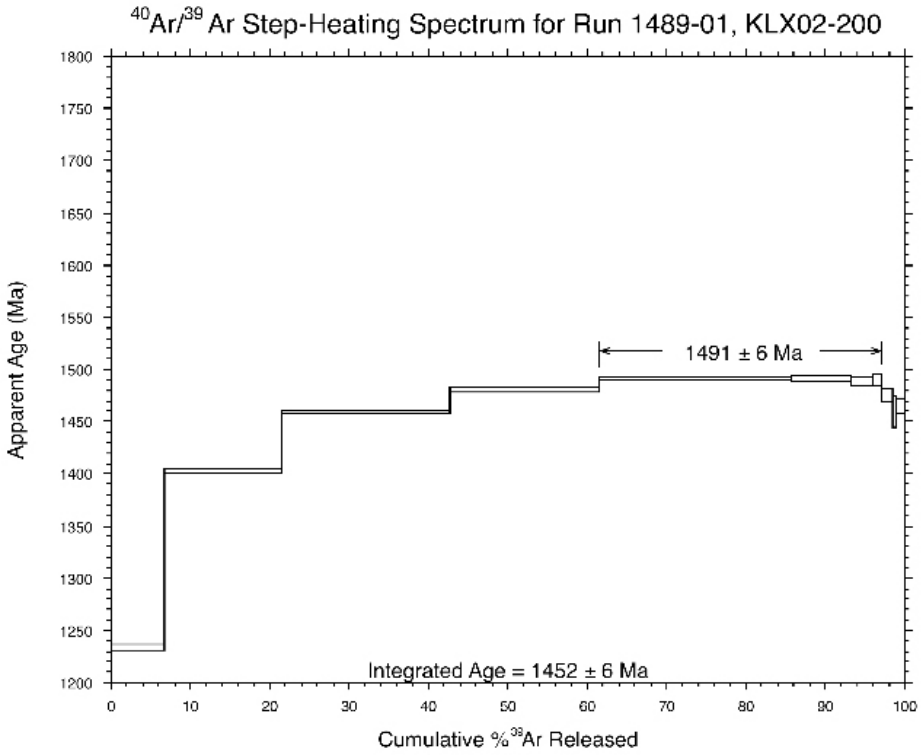

Figure 5-7. *$^{40}Ar/^{39}Ar$ biotite step-heating spectrum for sample KLX02-200.*

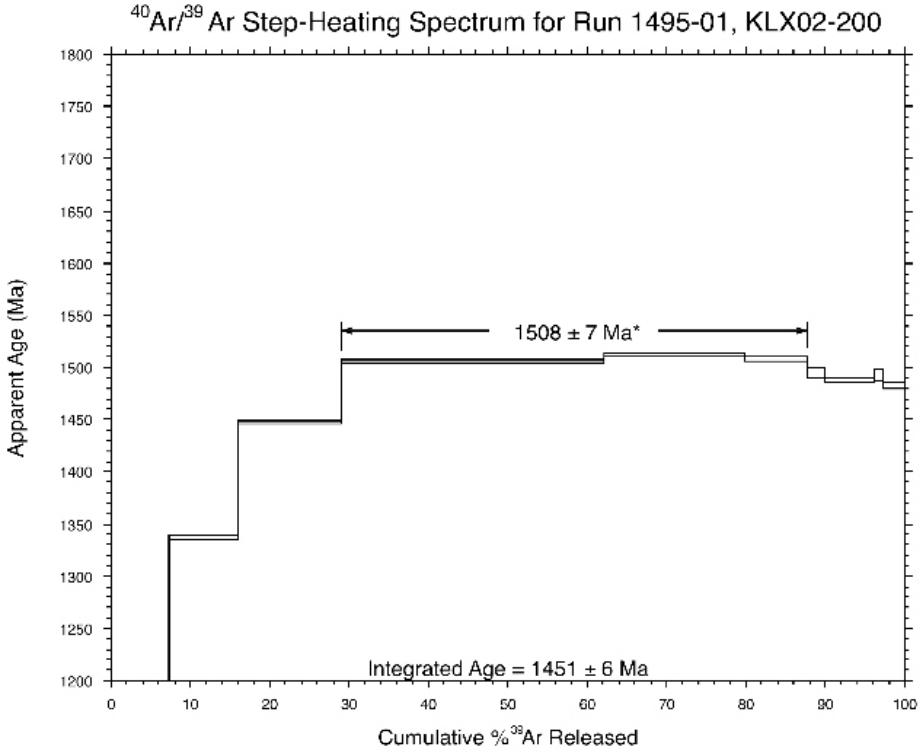

Figure 5-8. *$^{40}Ar/^{39}Ar$ biotite step-heating spectrum for sample KLX02-200.*

KLX02-1600

The $^{40}Ar/^{39}Ar$ age for biotite from Ävrö granite that was sampled in the interval 1,604.85–1,605.39 m (borehole length) can be seen in Figure 5-9. The plateau age, 1,431 ± 6 Ma, is interpreted as dating the cooling below the closure temperature of biotite (c 300°C).

The $^{40}Ar/^{39}Ar$ age versus depth profiles for amphibole and biotite from KLX02 are provided below in Figures 5-10 and 5-11, respectively. These are discussed further in the conclusions section. The red band indicates deformation zone according to the geological single-hole interpretation.

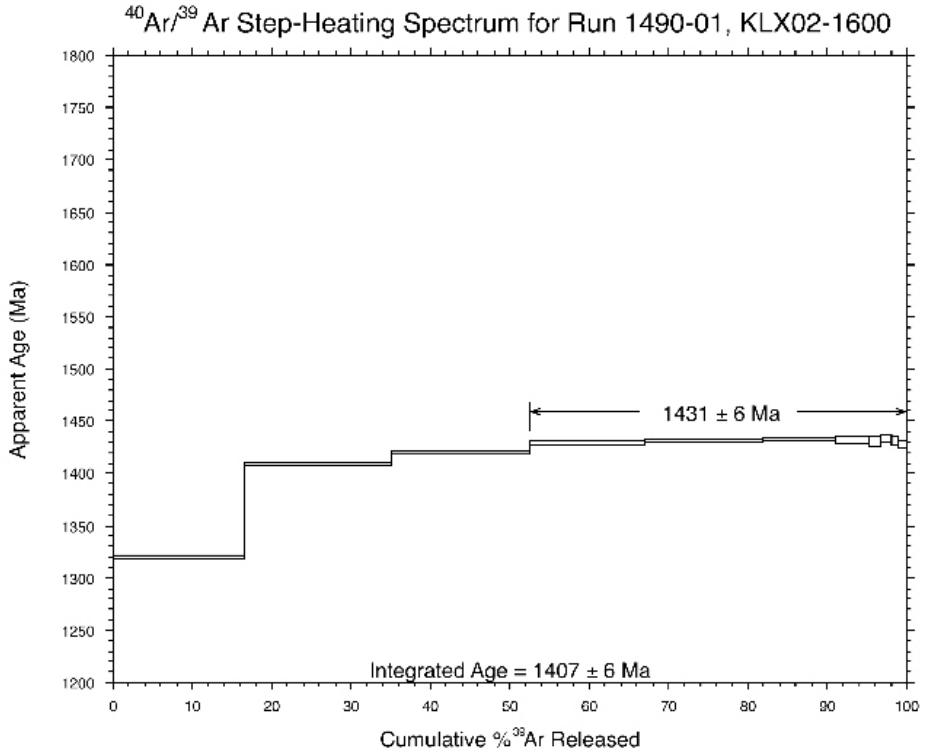

Figure 5-9. *$^{40}Ar/^{39}Ar$ biotite step-heating spectrum for sample KLX02-1600.*

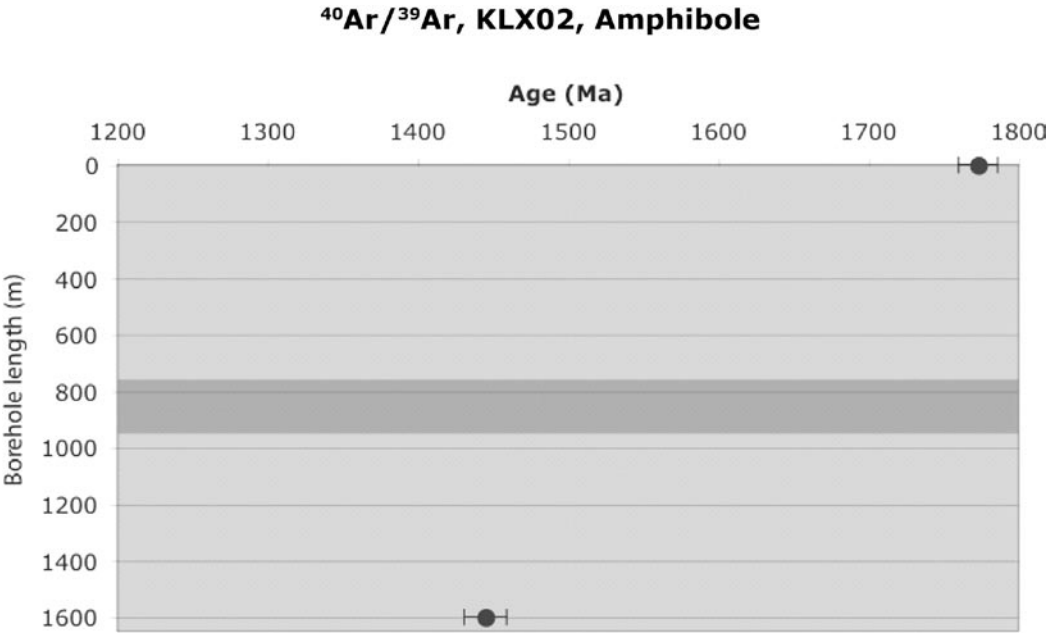

Figure 5-10. *$^{40}Ar/^{39}Ar$ amphibole age vs borehole length profile from KLX02 including surface sample PSM000026. The red band marks an identified deformation zone from the geological single-hole interpretation.*

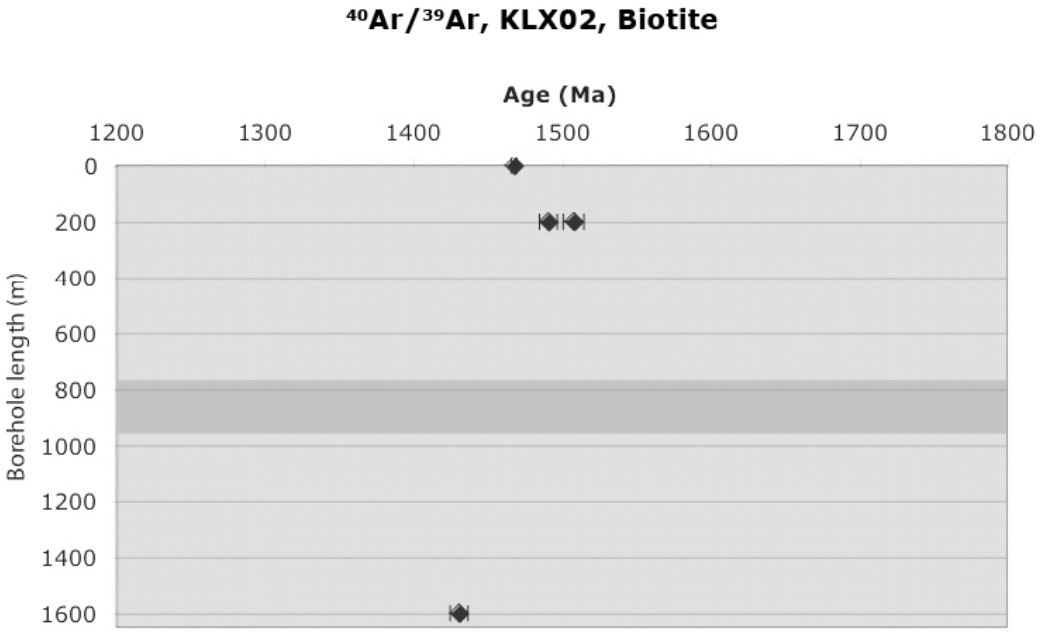

Figure 5-11. *$^{40}Ar/^{39}Ar$ biotite age vs borehole length profile from KLX02 including surface sample PSM000026. The red band marks an identified deformation zone from the geological single-hole interpretation*

KSH03A/B

KSH03A-127

The $^{40}Ar/^{39}Ar$ age of amphibole from quartz monzodiorite that was sampled in the interval 126.7–126.9 m (borehole length) in KSH03A can be seen in Figure 5-12. The plateau age, 1,799 ± 4 Ma, is interpreted as dating the cooling below the closure temperature of amphibole (c 500°C).

KSH03B-4

Two $^{40}Ar/^{39}Ar$ biotite samples from quartz monzodiorite that was sampled in the interval 3.95–4.15 m (borehole length) in KSH03B were analysed. A forced plateau age of 1,618 ± 7 Ma (Figure 5-13) and a plateau age of 1,621 ±3 (Figure 5-14) were obtained and are interpreted as dating the cooling below the closure temperature of biotite (c 300°C).

KSH03A-127

$^{40}Ar/^{39}Ar$ dating of biotite from the quartz monzodiorite yielded no interpretable age (Figure 5-15).

KSH03A-300

The $^{40}Ar/^{39}Ar$ age of biotite from Ävrö granite that was sampled in the interval 308.12–308.32 m (borehole length) can be seen in Figure 5-16. A three step plateau age, 928 ± 6 Ma, is interpreted as dating the cooling below the closure temperature of biotite (c 500°C) although it must be considered that the spectra is quite disturbed.

KSH03A-1000

Two $^{40}Ar/^{39}Ar$ biotite samples were analysed from Ävrö granite that was sampled in the interval 999.6–999.9 m (borehole length). A plateau age of 1,484 ± 3 Ma (Figure 5-17) and a plateau age of 1,479 ± 3 Ma (Figure 5-18) were obtained and is interpreted as dating the cooling below the closure temperature of biotite (c 300°C).

The $^{40}Ar/^{39}Ar$ age versus depth profiles for KSH03A/B is provided below for amphibole and biotite in Figure 5-19 and Figure 5-20, respectively. These are discussed further in the conclusions section.

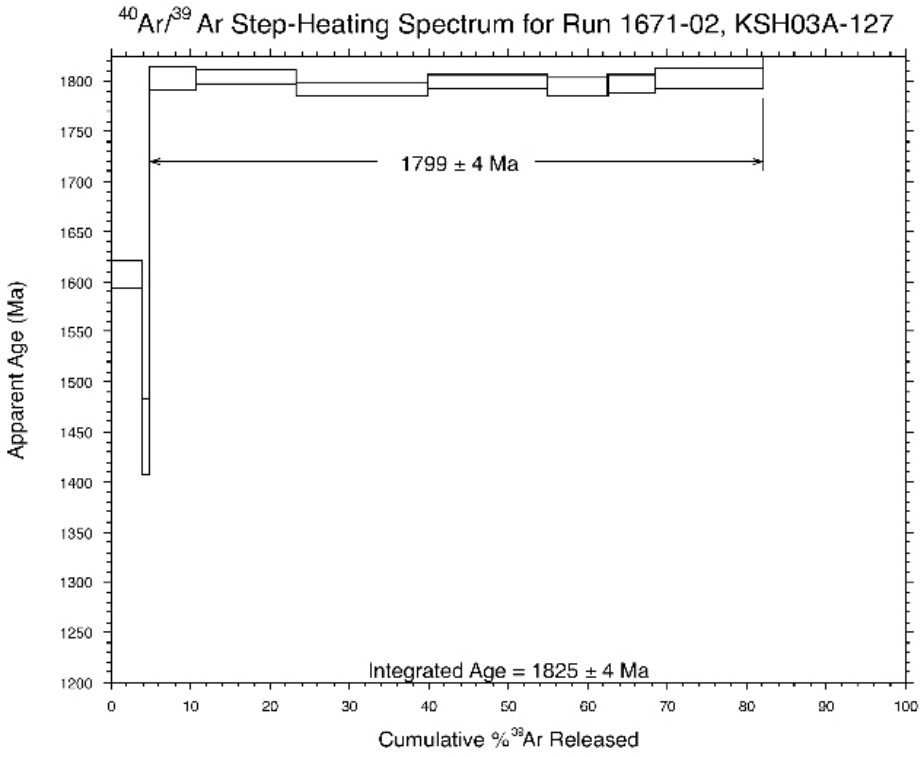

Figure 5-12. *$^{40}Ar/^{39}Ar$ amphibole step-heating spectrum for sample KSH03A-127.*

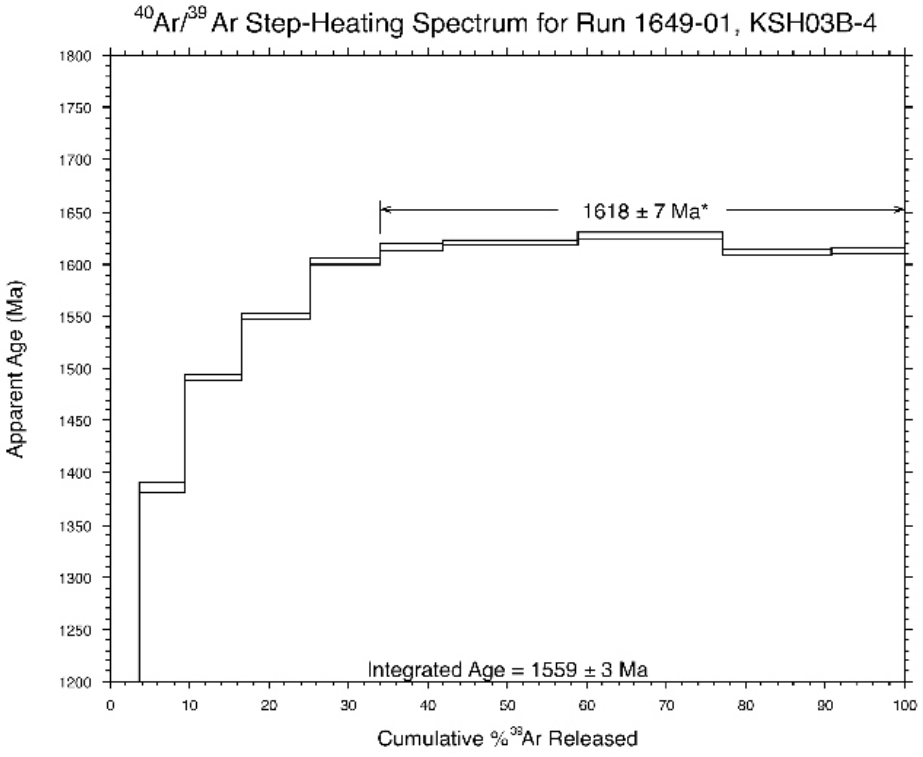

Figure 5-13. *$^{40}Ar/^{39}Ar$ biotite step-heating spectrum for sample KSH03B-4.*

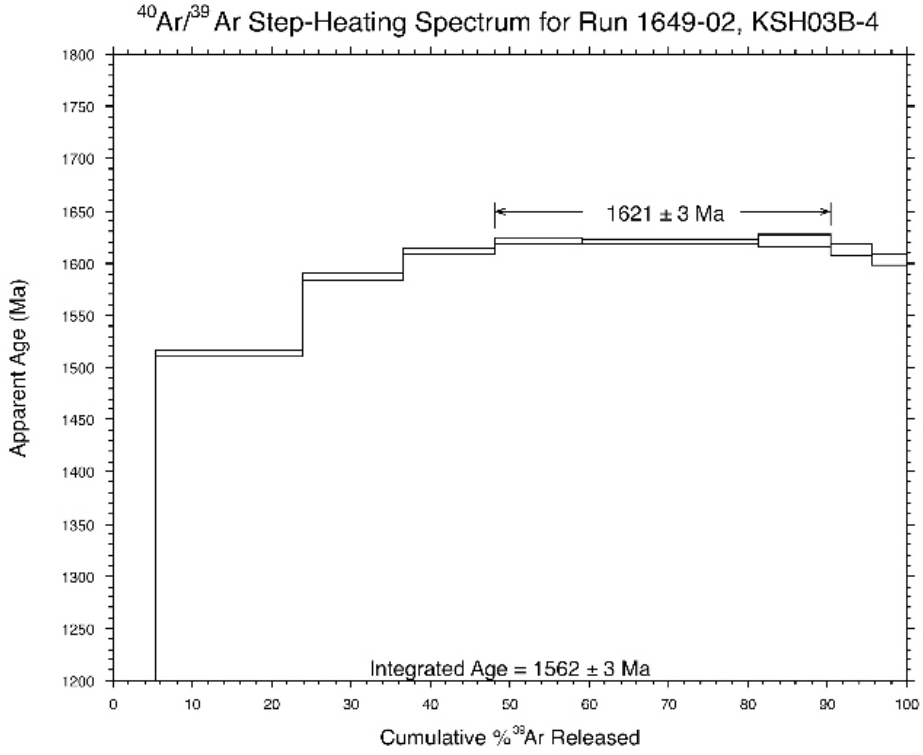

Figure 5-14. *$^{40}Ar/^{39}Ar$ biotite step-heating spectrum for sample KSH03B-4.*

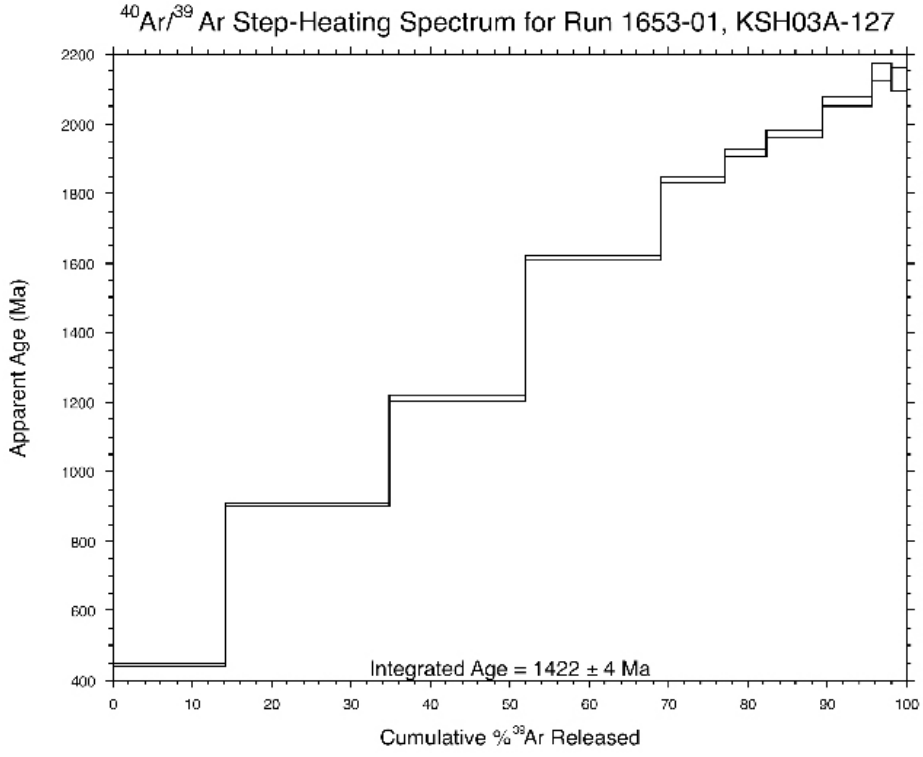

Figure 5-15. *$^{40}Ar/^{39}Ar$ biotite step-heating spectrum for sample KSH03A-127.*

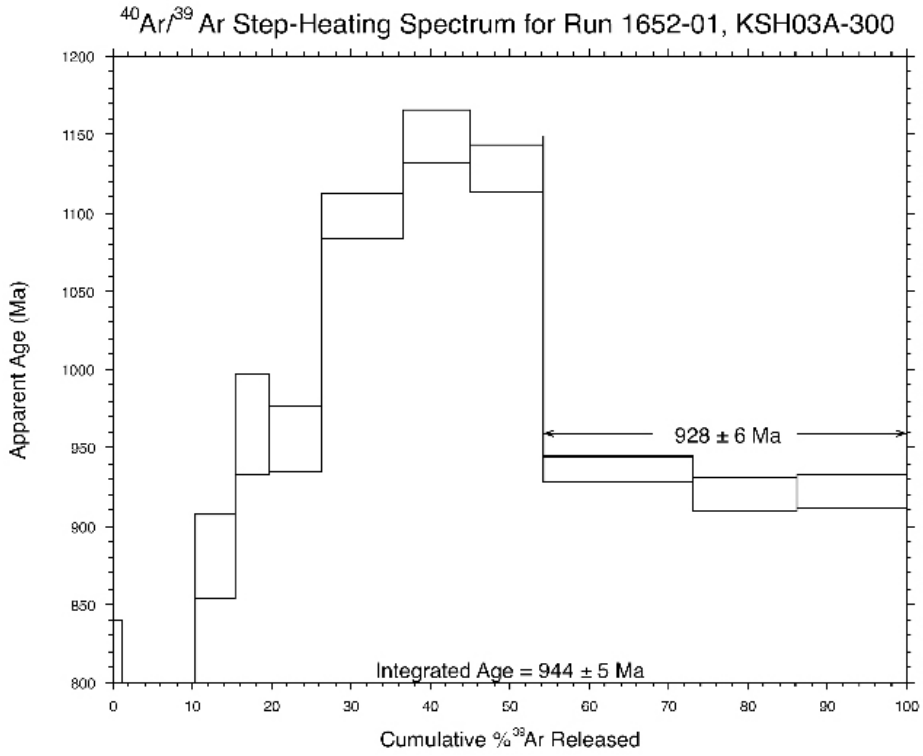

Figure 5-16. *$^{40}Ar/^{39}Ar$ biotite step-heating spectrum for sample KSH03A-300.*

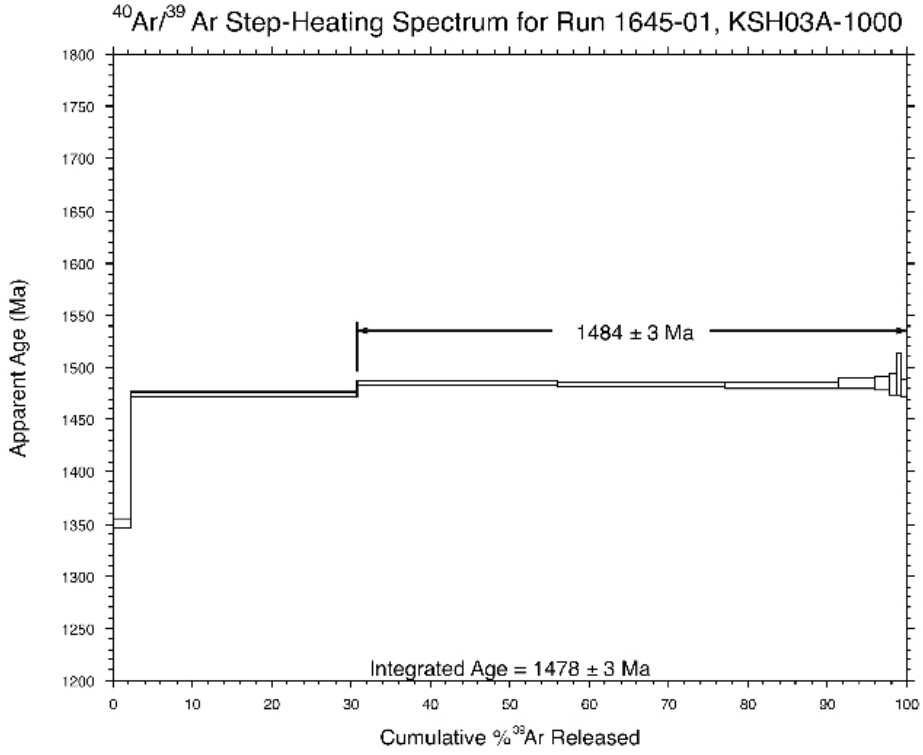

Figure 5-17. *$^{40}Ar/^{39}Ar$ biotite step-heating spectrum for sample KSH03A-1000.*

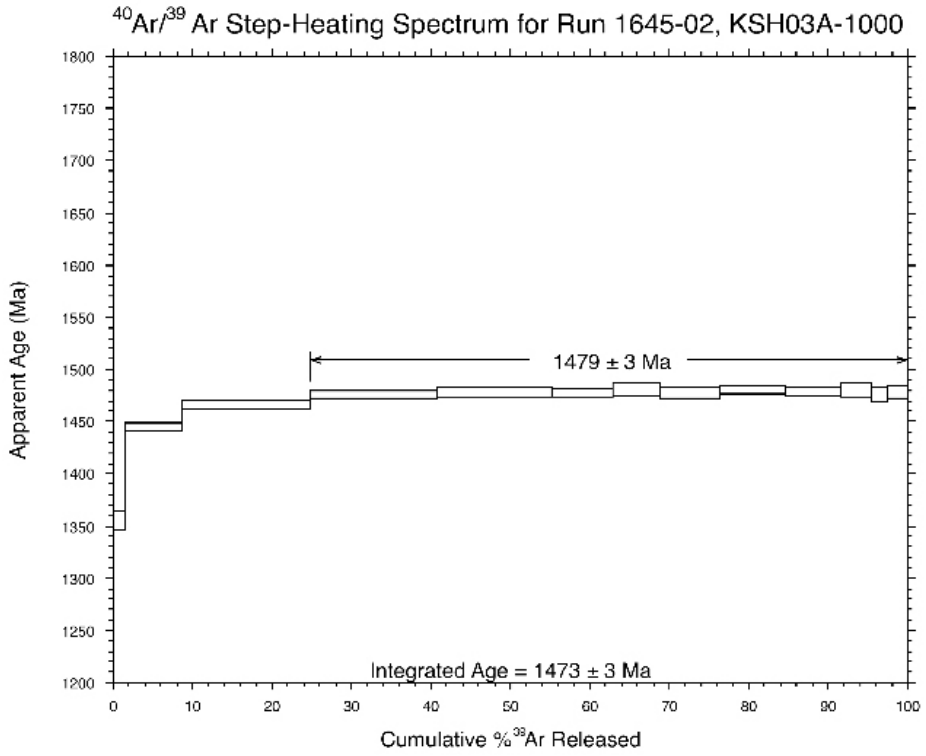

Figure 5-18. *$^{40}Ar/^{39}Ar$ biotite step-heating spectrum for sample KSH03A-1000.*

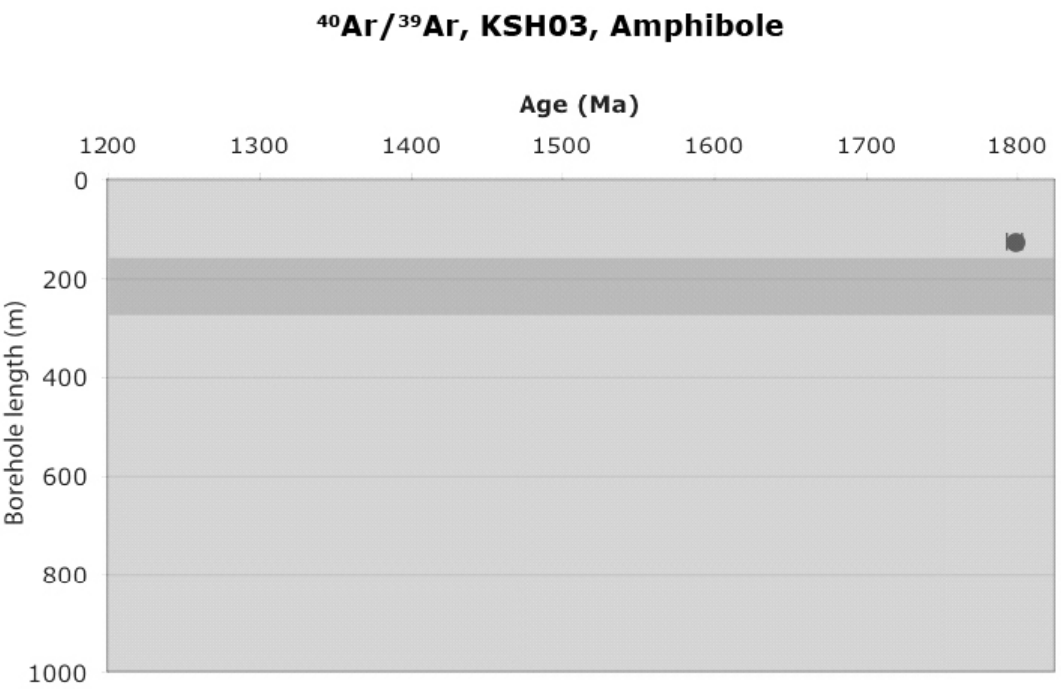

Figure 5-19. *$^{40}Ar/^{39}Ar$ amphibole age vs borehole length profile from KSH03. The red band marks an identified deformation zone from the geological single-hole interpretation.*

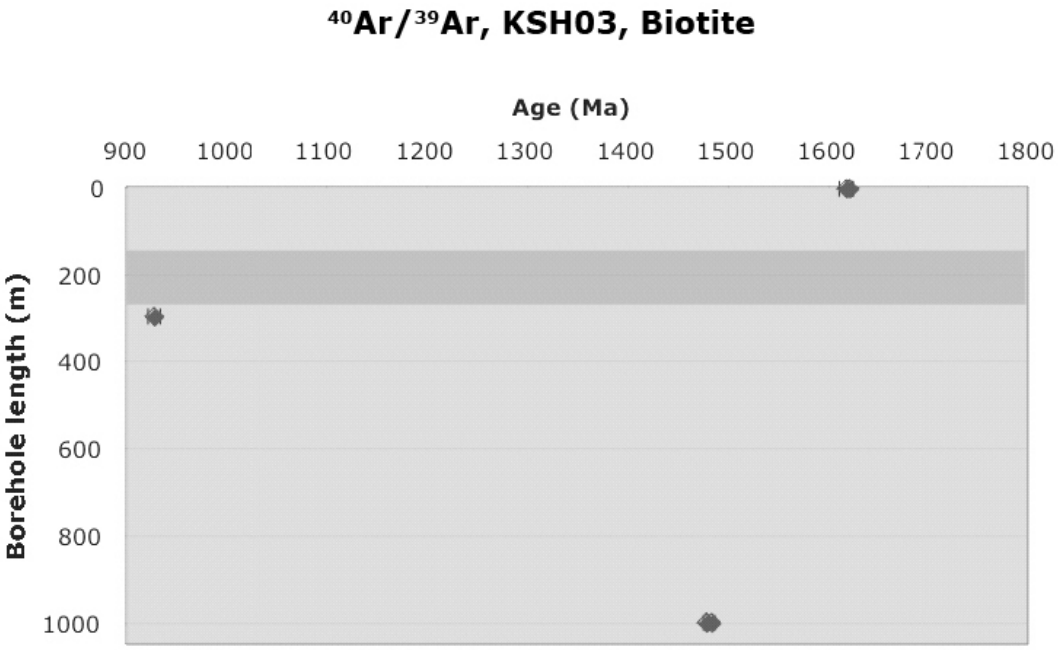

Figure 5-20. *$^{40}Ar/^{39}Ar$ biotite age vs borehole length profile from KSH03A/B. The red band marks an identified deformation zone from the geological single-hole interpretation.*

Discussion

The data from the drill cores from KSH03A/B, KLX01 and KLX02, including the surface sample close to KLX02, reveal a tectonothermal history that was previously only partly known or suggested. The amphibole ages of 1,799 ± 5 Ma and 1,773 ± 13 Ma are interpreted to be related to the intrusion of the c 1,800 Ma TIB rocks, i.e. the Ävrö granite and quartz monzodiorite, that characterize the area. The 1,621 ± 3 Ma biotite age may be interpreted as a cooling age also related to the protolith. The amphibole and biotite ages indicate an initially fast cooling followed by much slower cooling, which is in agreement with other studies /e.g. Dörr et al. 2002/.

Including three surface samples collected from an independent study (Figure 5-21), the younger biotite ages, i.e. < c 1,510 Ma, can be divided into two different groups: one at c 1,468–1,508 Ma and the other at c 1,419–1,434 Ma, plus an amphibole age of c 1,445 Ma, which has been grouped with the younger interval. $^{40}Ar/^{39}Ar$ amphibole ages of c 1,570–1,470 Ma has been reported from the Loftahammar-Linköping Deformation Zone (LLDZ) (Page unpublished results), some 200 km north of Oskarshamn. Additionally, /Page et al. 2006/ recently dated biotite from south of Norrköping to 1,493 ± 6 Ma. These ages can possibly be linked to the younger phase of the peripheral rapakivi intrusions (see for example Figure 8 in /Dörr et al. 2002/). The Götemar and Uthammar granites are considered to be different and not belong to these intrusions.

The younger group of biotite ages (1,419–1,434 Ma) plus one amphibole age (1,445 Ma) are probably linked to the intrusions of the Götemar and Uthammar granites. Three analysed samples taken in connection with another research project not related to SKB help shed some light on the interpretion of the area (unpublished data). One sample (O0102) taken from within the Götemar granite yields perfect plateau ages of c 1,423 ± 6 Ma and 1,419 ± 6 Ma with virtually no signs of Ar-loss. The weighted average of these two ages is 1,421 ± 4 Ma, which is the age interpreted to reflect cooling through 300°C of the intrusion. Another sample (O0103) is from the very vicinity of the Uthammar granite. Close to 100% of the total ^{39}Ar-gas release define the plateau of this sample and, thus, the age of 1,434 ± 6 Ma must indicate cooling of either newly formed biotite in a restricted area close to the Uthammar intrusion or complete reset of the older biotite in the rock. Either way, it is reasonable to assume that at the vicinity of the intrusion the heat decays faster than within the intrusion. Therefore the cooling age is closer in time to the actual intrusion (a difference of only 6 Ma) than when the sample is from

the intrusion itself, where the difference is c 30 Ma. At the bottom of KLX02 the amphibole age is 1,445 ± 15 Ma and the biotite age is 1,431 ± 6 Ma. Since the southern contact of the Götemar intrusion is interpreted to dip to the south /SKB 2006; Wahlgren et al. 2006 /, the bottom of KLX02 is close to the intrusion (Figure 5-22). The ages possibly reflect resetting of both amphibole and biotite, whereas samples further away, e.g. at 1,000 m depth of KLX01, yield ages older than the intrusion and are interpreted as not being affected by the intrusion.

Another possible interpretation is that all ages refer to the Götemar and Uthammar intrusions. With increasing distance from the intrusions, samples would have decreasing tendency to reach complete reset with a result in vast ages spread. Even plateau ages that are older than the actual intrusions could be explained by saying that the biotites in these samples reflect a much lower degree of resetting and therefore yield higher ages. However, we find it hard to explain why partly reset biotite ages would be separated into two well-defined age intervals.

In KSH03A/B the biotite ages vary throughout the drill core; 1,621 ± 3 Ma at the top, 1,479 ± 3 Ma at the bottom and poorly defined ages at 127 m and 300 m. Of all the analysed samples, the top of KSH03 is the only biotite sample that yields an age older than c 1,500 Ma. Consequently, neither any thermal heat at c 1,500 Ma, nor the Götemar or Uthammar intrusions had strong enough impact to reset the biotites in this sample. This could be explained either by less distributed heat in this local area or by claiming that the rock at the surface of KSH03B has been transported to its present position sometime after 1,450 Ma. The borehole crosses a prominent deformation zone (ZSMNE024A) /SKB 2006; Wahlgren et al. 2006/ that shows signs of having a complicated history. The zone displays both low-grade ductile as well has brittle (dominating) deformation. The disturbed Ar-biotite spectra from samples at the border of the zone provide further support for activity. The biotite age of 928 ± 6 Ma from the sample at c 300 m borehole length may indicate disturbance during the Sveconorwegian event, active some 200 km west of Oskarshamn. /Drake et al. 2006/ recently dated adularia from the zone with $^{40}Ar/^{39}Ar$ yielding an age of 401 ± 1 Ma. Another, smaller fracture zone at c 860 m borehole length yields an $^{40}Ar/^{39}Ar$ adularia age of 989 ± 2Ma /Drake et al. 2006/. This indicates that hot fluids, or other parameters causing resetting such as frictional heating due to movement, have interacted in zones at several occasions. The spectra from both 127 m of this drill core and from the surface sample O0101 also indicate disturbed minerals, which could be explained by closeness to deformation zones.

Conclusions

- Surface amphibole ages of 1,773 ± 13 and 1,799 ± 4 Ma indicate initial fast cooling of the c 1,800 Ma TIB rocks followed by slower cooling shown by c 1,620 Ma biotite ages.
- The $^{40}Ar/^{39}Ar$ isotopic system in biotite has been reset at c 1,510–1,470 Ma in the Oskarshamn area. This resetting may have been caused by the anorogenic rapakivi event at 1,645–1,470 Ma, which affected a large area of the crust.
- The Götemar and Uthammar intrusions appears to have had major thermal effects on rocks in their immediate surrounding causing resetting of the $^{40}Ar/^{39}Ar$ isotopic system in both biotite and amphibole after the first resetting at c 1,510–1,470 Ma.
- Movements along deformation zones may have occurred after 1,470 Ma. There are indications for a Sveconorwegian resetting of the $^{40}Ar/^{39}Ar$ isotopic system in biotite in the deformation zone in KSH03A (ZSMNE0024A).

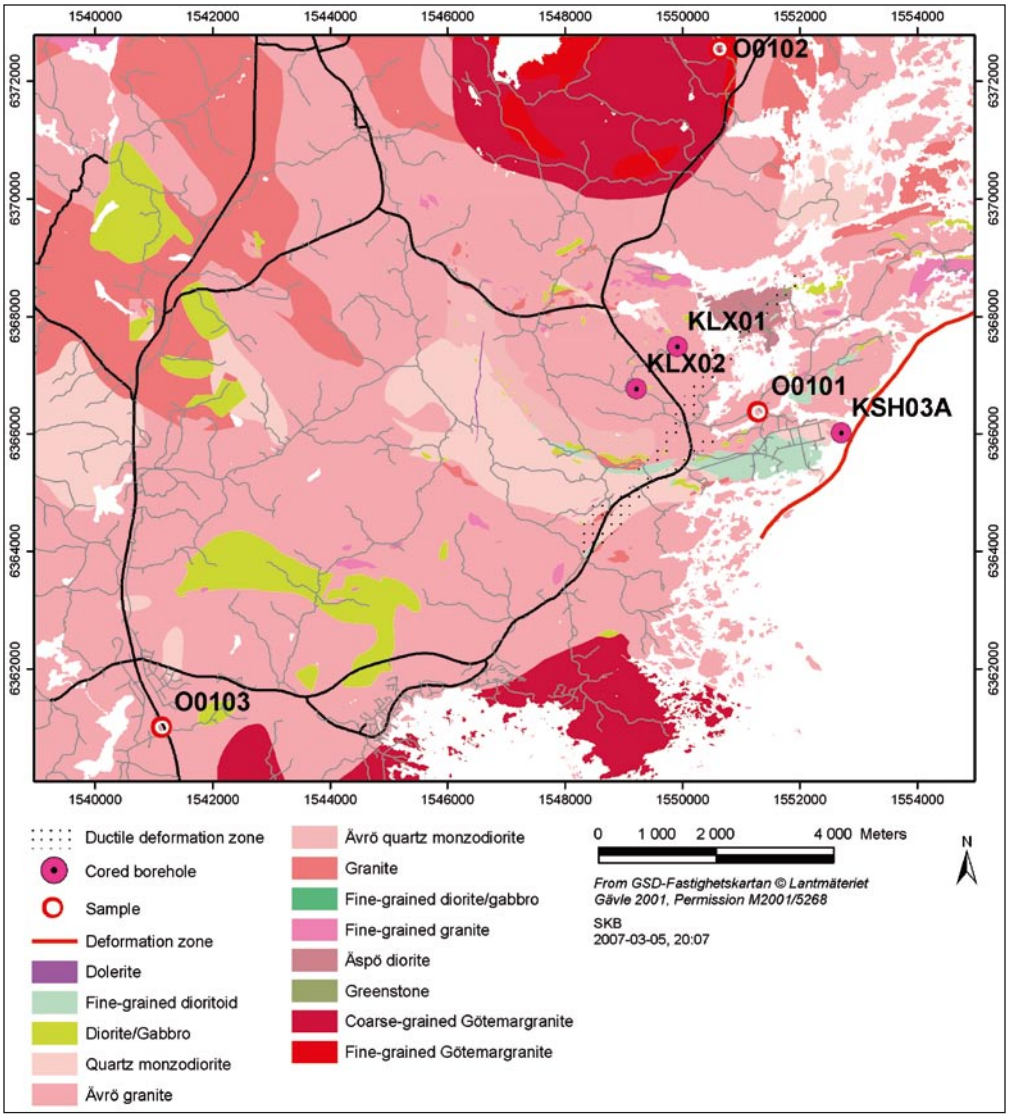

Figure 5-21. *Sample locations for surface samples O0101, O0102 and O0103 from an independent study.*

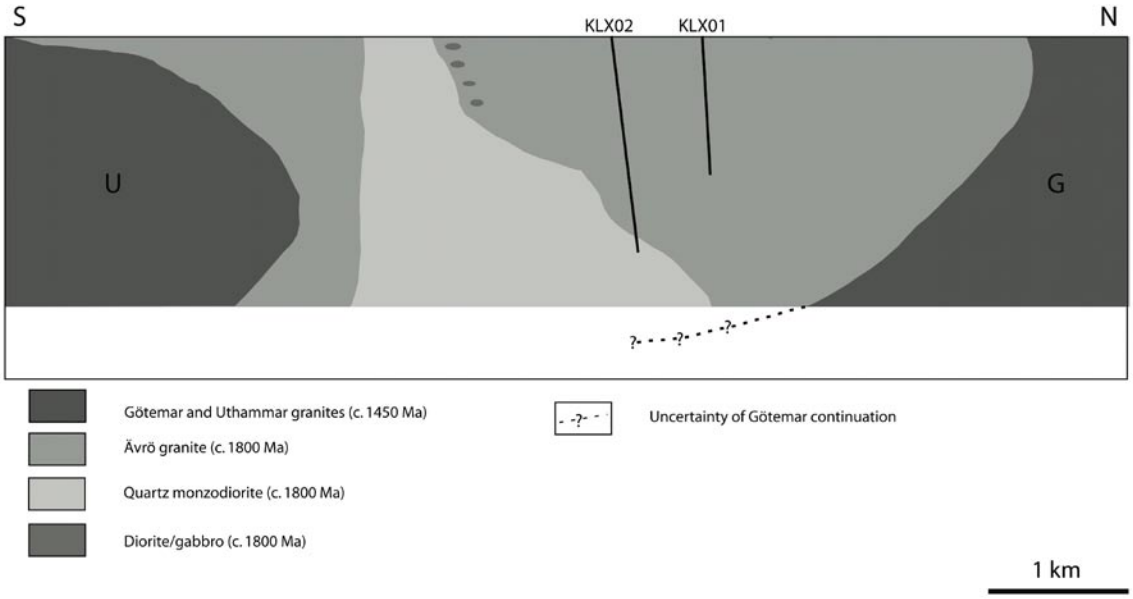

Figure 5-22. *Cross-section showing relationship at depth of boreholes and the Götemar and Uthammar ranites according to the Laxemar 1.2 rock domain model /SKB 2006; Wahlgren et al. 2006/.*

Table 5-1. $^{40}Ar/^{39}Ar$ amphibole data.

Sample ID/Run ID	Power (W)	Ca/K	Cl/K	$^{36}Ar/^{39}Ar$	$\%^{36}Ar(Ca)$	$^{40}Ar^*/^{39}Ar$	^{39}Ar (Mol-14)	$\%^{39}Ar$	Cum. $\%^{39}Ar$	$\%^{40}Ar^*$	Age (Ma)	± 2σ
PSM000026, Run ID# 1673-01 (J = 0.01063 ± 0.000012), Amphibole:												
1673–01A	1.6	49.97	4.65	0.793	0.9	220.893	0.0003	0.1	0.1	48.3	2,180.03	455.42
1673–01B	1.7	0.21	0.11	0.003	1.1	179.522	0.0084	1.6	1.6	99.6	1,925.99	20.05
1673–01C	1.8	2.18	0.16	0.054	0.6	124.376	0.0031	0.6	2.2	88.8	1,519.90	46.52
1673–01D	1.9	1.01	0.01	0.013	1.1	178.788	0.0017	0.3	2.5	98	1,921.14	86.33
1673–01E	1.9	4.79	0.17	0.029	2.3	119.753	0.0031	0.6	3.1	93.5	1,481.31	43.87
1673–01F	2	19.30	0.27	0.100	2.7	135.807	0.0012	0.2	3.3	82.5	1,611.91	100.27
1673–01G	2	7.42	0.20	0.059	1.7	117.120	0.0024	0.4	3.8	87.2	1,458.96	50.03
1673–01H	2.1	0.53	0.00	0.007	1.1	158.401	0.0032	0.6	4.4	98.8	1,781.05	43.31
1673–01I	•2.2	0.19	0.23	0.007	0.4	155.796	0.0450	8.4	12.8	98.8	1,762.34	4.48
1673–01J	•2.3	0.08	0.34	0.001	1.9	156.606	0.2226	41.5	54.2	99.9	1,768.18	2.38
1673–01K	•2.5	0.14	0.30	0.000	4.7	159.126	0.1799	33.5	87.7	99.9	1,786.22	2.58
1673–01L	•4.0	0.35	0.29	0.004	1.3	154.568	0.0659	12.3	100	99.3	1,753.45	5.18
Integ. Age=											1,771.00	4.00
(•) Plateau Age =								95.6			1,773.00	13.00
KLX02–1600, Run ID# 1672–01 (J = 0.01063 ± 0.000012), Amphibole:												
1672–01A	1.6	1.18	0.02	0.006	2.6	137.108	0.0054	1.7	1.7	98.7	1,622.09	25.71
1672–01B	1.7	0.42	0.01	0.027	0.2	94.670	0.0062	1.9	3.6	92.3	1,256.20	21.91
1672–01C	1.8	0.15	0.04	0.009	0.2	107.403	0.0133	4.1	7.6	97.7	1,373.98	11.37
1672–01D	1.9	0.56	0.09	0.018	0.4	113.441	0.0102	3.1	10.8	95.4	1,427.25	13.87
1672–01E	1.9	0.19	0.04	0.042	0.1	116.787	0.0030	0.9	11.7	90.4	1,456.11	44.24
1672–01F	2	1.41	0.01	0.015	1.3	170.748	0.0016	0.5	12.2	97.5	1,867.18	80.45
1672–01G	2	0.50	0.17	0.006	1.2	129.322	0.0044	1.3	13.5	98.7	1,560.29	32.58
1672–01H	2.1	3.68	0.02	0.020	2.5	118.335	0.0043	1.3	14.8	95.3	1,469.31	35.78
1672–01I	•2.2	0.16	0.25	0.000	7.1	116.897	0.0842	25.7	40.6	99.9	1,457.05	2.90
1672–01J	•2.3	0.60	0.18	0.015	0.6	111.492	0.0202	6.2	46.7	96.3	1,410.23	8.56
1672–01K	•2.5	0.03	0.23	0.000	1.1	115.074	0.0809	24.7	71.5	99.9	1,441.40	3.13
1672–01L	•4.0	0.19	0.26	0.003	0.8	114.580	0.0932	28.5	100	99.2	1,437.13	3.53
Integ. Age=											1,444.00	5.00
(•) Plateau Age =								85.2			1,445.00	14.00
KSH03A–127, Run ID# 1671–02 (J = 0.01063 ± 0.000012), Amphibole:												
1671–02A	1.6	0.29	0.14	0.049	0.1	135.114	0.0292	3.9	3.9	90.3	1,606.47	6.90
1671–02B	1.7	0.45	0.25	0.023	0.3	115.577	0.0071	1	4.9	94.4	1,445.72	19.03
1671–02C	•1.8	0.73	0.93	0.005	1.9	161.425	0.0443	5.9	10.8	99.1	1,802.53	5.58
1671–02D	•1.9	0.06	0.96	0.004	0.2	161.656	0.0938	12.5	23.3	99.3	1,804.16	3.38
1671–02E	•1.9	0.24	0.94	0.003	1	160.037	0.1237	16.5	39.9	99.4	1,792.70	3.48
1671–02F	•2.0	0.13	0.88	0.003	0.6	161.044	0.1121	15	54.9	99.5	1,799.83	3.34
1671–02G	•2.0	0.10	0.90	0.003	0.5	160.335	0.0567	7.6	62.4	99.5	1,794.81	4.47
1671–02H	•2.1	0.21	0.89	0.008	0.4	160.664	0.0451	6	68.5	98.6	1,797.15	4.74
1671–02I	•2.2	0.04	0.93	0.004	0.1	161.489	0.1014	13.6	82	99.3	1,802.98	5.22
1671–02J	2.3	0.21	1.06	0.005	0.5	172.050	0.0854	11.4	93.4	99.1	1,876.03	3.94
1671–02K	4	0.03	1.45	0.012	0	220.384	0.0490	6.6	100	98.4	2,177.11	5.63
Integ. Age=											1,825.00	4.00
(•) Plateau Age =								77.2			1,799.00	5.00

Table 5-2. $^{40}Ar/^{39}Ar$ biotite data.

Sample ID/Run ID#	Power (W)	Ca/K	Cl/K	$^{36}Ar/^{39}Ar$	$\%^{36}Ar(Ca)$	$^{40}Ar^*/^{39}Ar$	^{39}Ar (Mol-14)	$\%^{39}Ar$	Cum. $\%^{39}Ar$	$\%^{40}Ar^*$	Age (Ma)	± 2σ
KLX01–5, Run ID# 1646–01 (J = 0.01063 ± 0.000012):												
1646–01A	1.4	0.08	0.057	0.653	0	75.095	0.00181	0.2	0.2	28	1,058.67	17.45
1646–01B	1.6	0.08	0.016	0.096	0	74.641	0.01379	1.2	1.4	72.4	1,053.82	3.14
1646–01C	1.8	0.00	0.027	0.013	0	117.784	0.19124	17	18.4	96.9	1,464.62	1.03
1646–01D	•2.0	0.02	0.028	0.001	0.2	120.095	0.18792	16.7	35.1	99.7	1,484.19	1.33
1646–01E	•2.2	0.02	0.027	0.001	0.3	120.534	0.23039	20.5	55.6	99.8	1,487.88	5.28
1646–01F	•2.4	0.01	0.027	0.000	0.5	120.465	0.19012	16.9	72.5	99.9	1,487.30	1.48
1646–01G	•2.6	0.06	0.026	0.000	13.8	120.564	0.11088	9.9	82.3	100	1,488.13	1.38
1646–01H	•2.8	0.20	0.026	0.001	2.9	120.079	0.08163	7.3	89.6	99.8	1,484.06	1.30
1646–01I	•3.0	0.47	0.025	0.001	6.7	120.474	0.04838	4.3	93.9	99.8	1,487.38	1.76
1646–01J	•3.4	0.98	0.027	0.000	211.8	120.214	0.06302	5.6	99.5	100	1,485.19	1.50
1646–01K	•3.9	0.32	-0.011	0.001	3.2	120.913	0.00599	0.5	100	99.7	1,491.07	8.42
Integ. Age=											1,477.00	3.00
(•) Plateau Age =								81.6			1,486.00	3.00
KLX01–1000, Run ID# 1650–01 (J = 0.01063 ± 0.000012):												
1650–01A	1.5	0.16	0.023	0.051	0	37.144	0.02565	4.1	4.1	71.2	600.37	2.86
1650–01B	1.7	0.03	0.024	0.019	0	109.655	0.09248	14.9	19.1	95.1	1,394.04	1.20
1650–01C	1.8	0.03	0.021	0.001	0.3	115.853	0.05999	9.7	28.7	99.7	1,448.10	1.70
1650–01D	1.9	0.03	0.022	0.001	0.4	118.419	0.05532	8.9	37.7	99.7	1,470.02	1.36
1650–01E	•2.0	0.05	0.021	0.001	0.6	119.674	0.03904	6.3	44	99.7	1,480.64	1.79
1650–01F	•2.1	0.06	0.019	0.001	0.7	119.436	0.03770	6.1	50.1	99.7	1,478.63	1.74
1650–01G	•2.2	0.06	0.022	0.001	0.8	121.054	0.07981	12.9	62.9	99.8	1,492.25	9.80
1650–01H	•2.3	0.08	0.022	0.002	0.7	120.188	0.06232	10.1	73	99.6	1,484.98	1.57
1650–01I	•2.4	0.06	0.025	0.000	162.4	119.592	0.04000	6.5	79.5	100	1,479.95	1.53
1650–01J	•2.6	0.11	0.020	0.001	1.1	119.753	0.02842	4.6	84	99.7	1,481.31	1.91
1650–01K	3	0.04	0.021	0.000	13.4	117.212	0.04686	7.6	91.6	100	1,459.75	1.47
1650–01L	3.5	0.15	0.025	0.001	1.5	116.415	0.03262	5.3	96.9	99.7	1,452.93	1.89
1650–01M	5	0.18	0.014	0.001	1.7	116.672	0.01944	3.1	100	99.7	1,455.12	2.58
Integ. Age=											1,432.00	4.00
(•) Plateau Age =								46.4			1,481.00	3.00
PSM000026, Run ID# 1647–01 (J = 0.01063 ± 0.000012):												
1647–01A	1.4	0.07	–0.004	0.167	0	58.356	0.00692	0.4	0.4	54.1	870.69	5.85
1647–01B	1.6	0.02	0.018	0.028	0	100.536	0.06844	4.4	4.8	92.5	1,311.42	1.30
1647–01C	1.8	0.01	0.021	0.006	0	116.214	0.23875	15.2	20	98.4	1,451.20	1.15
1647–01D	•2.0	0.01	0.021	0.001	0.1	118.402	0.24956	15.9	35.9	99.7	1,469.87	1.29
1647–01E	•2.2	0.00	0.021	0.001	0	117.998	0.37151	23.6	59.5	99.8	1,466.44	1.15
1647–01F	•2.4	0.02	0.021	0.001	0.4	118.211	0.26279	16.7	76.2	99.9	1,468.25	1.05
1647–01G	•2.6	0.03	0.022	0.000	1.2	118.184	0.18029	11.5	87.7	99.9	1,468.02	1.33
1647–01H	•2.8	0.09	0.020	0.001	1.3	118.293	0.08175	5.2	92.9	99.8	1,468.95	1.52
1647–01I	•3.0	0.42	0.017	0.001	5.1	118.484	0.04729	3	95.9	99.7	1,470.57	2.15
1647–01J	•3.4	0.75	0.018	0.001	7.8	118.026	0.05018	3.2	99.1	99.7	1,466.68	1.57
1647–01K	•3.9	0.48	0.005	0.002	2.8	118.095	0.01110	0.7	99.8	99.4	1,467.27	4.68
1647–01L	•4.5	0.98	0.064	0.011	1.3	116.851	0.00265	0.2	100	97.4	1,456.66	16.89
Integ. Age=											1,457.00	3.00
(•) Plateau Age =								80			1,468.00	2.00

Sample ID/Run ID#	Power (W)	Ca/K	Cl/K	$^{36}Ar/^{39}Ar$	$\%^{36}Ar(Ca)$	$^{40}Ar^*/^{39}Ar$	^{39}Ar (Mol-14)	$\%^{39}Ar$	Cum. $\%^{39}Ar$	$\%^{40}Ar^*$	Age (Ma)	± 2σ
KLX02–200, Run ID# 1489–01 (J = 0.009461 ± 0.000029):												
1489–01A	1.7	7.24	0.008	3.890	0	50.326	0.00010	0	0	4.2	702.56	134.96
1489–01B	1.8	0.02	0.010	0.096	0	103.730	0.02899	6.7	6.7	78.5	1,233.63	1.35
1489–01C	1.9	0.04	0.971	0.014	0	124.272	0.06372	14.8	21.5	96.9	1,402.43	0.95
1489–01D	2	0.07	0.975	0.003	0.4	131.573	0.09148	21.2	42.7	99.4	1,458.82	0.71
1489–01E	2.1	0.00	0.974	0.001	0	134.400	0.08175	18.9	61.6	99.7	1,480.18	0.88
1489–01F	•2.2	0.05	0.976	0.001	0.5	135.880	0.10421	24.1	85.8	99.8	1,491.27	0.82
1489–01G	•2.4	0.14	0.010	0.002	1.2	135.922	0.03216	7.4	93.2	99.6	1,491.58	1.35
1489–01H	•2.6	0.08	0.010	0.002	0.6	135.490	0.01190	2.8	96	99.6	1,488.35	1.88
1489–01I	•2.8	1.31	0.013	0.001	13.5	135.656	0.00502	1.2	97.1	99.7	1,489.60	2.86
1489–01J	3.1	2.34	0.008	0.003	9.2	133.686	0.00573	1.3	98.4	99.3	1,474.81	2.95
1489–01K	3.5	2.34	0.028	0.006	5.3	131.692	0.00170	0.4	98.8	98.7	1,459.72	7.35
1489–01L	4.5	3.13	0.009	0.005	9.2	132.446	0.00500	1.2	100	99.1	1,465.44	3.59
Integ. Age=											1,452.00	6.00
(•) Plateau Age =								35.5			1,491.00	6.00
KLX02–200. Run ID# 1495–01 (J = 0.009461 ± 0.000029):												
1495–01A	1.7	53.68	0.047	0.564	1.3	52.569	0.00066	0.1	0.1	23.9	728.30	19.71
1495–01B	1.8	6.62	0.015	0.059	1.6	22.899	0.00627	1	1.1	57.3	353.78	2.53
1495–01C	1.9	0.14	0.010	0.111	0	90.910	0.03756	6.2	7.4	73.5	1,119.67	1.33
1495–01D	2	0.03	0.006	0.026	–0.1	116.027	0.05151	8.5	15.9	93.8	1,336.56	0.94
1495–01E	2.1	0.05	0.007	0.005	–0.1	130.104	0.07957	13.2	29.1	98.9	1,447.61	0.88
1495–01F	•2.2	0.17	0.007	0.002	1.1	137.801	0.19958	33.1	62.2	99.5	1,505.56	0.72
1495–01G	•2.4	0.16	0.006	0.002	1.3	138.579	0.10662	17.7	79.8	99.7	1,511.32	0.78
1495–01H	•2.6	0.03	0.005	0.001	0.2	138.140	0.04759	7.9	87.7	99.7	1,508.07	1.06
1495–01I	2.8	0.01	0.002	0.002	–6.6	136.342	0.01412	2.3	90	99.5	1,494.71	2.38
1495–01J	3.1	1.09	0.008	0.002	7.8	135.322	0.03689	6.1	96.2	99.6	1,487.10	1.06
1495–01K	3.5	0.05	0.005	0.002	–3.1	136.037	0.00643	1.1	97.2	99.5	1,492.44	2.89
1495–01L	4.5	0.27	0.008	0.002	2.3	134.740	0.01679	2.8	100	99.7	1,482.74	1.41
Integ. Age=											1,451.00	6.00
(•) Plateau Age =								58.6			1,508.00	7.00
KLX02–1600. Run ID# 1490–01 (J = 0.009461 ± 0.000029):												
1490–01A	1.7	35.43	0.081	1.628	0.3	76.497	0.00066	0.1	0.1	13.6	982.32	28.85
1490–01B	1.8	0.09	0.964	0.043	0	113.949	0.18157	16.4	16.5	90.1	1,319.58	0.85
1490–01C	1.9	0.01	0.973	0.007	0	125.145	0.20585	18.6	35.1	98.5	1,409.27	0.64
1490–01D	2	0.09	0.973	0.006	0.2	126.523	0.19291	17.4	52.5	98.7	1,420.01	0.80
1490–01E	•2.1	0.07	0.004	0.004	0.2	127.686	0.15883	14.4	66.9	99.1	1,429.02	0.81
1490–01F	•2.2	0.08	0.975	0.004	0.2	127.936	0.16716	15.1	82	99	1,430.95	0.76
1490–01G	•2.4	0.15	0.974	0.005	0.4	128.161	0.10013	9.1	91	98.9	1,432.69	1.08
1490–01H	•2.6	0.09	0.005	0.006	0.2	128.023	0.04496	4.1	95.1	98.6	1,431.62	1.72
1490–01I	•2.8	0.14	0.004	0.007	0.3	127.900	0.01887	1.7	96.8	98.3	1,430.67	2.67
1490–01J	•3.1	3.05	0.006	0.008	5	128.257	0.01318	1.2	98	98.2	1,433.42	1.62
1490–01K	•3.5	1.27	0.007	0.008	2.2	128.019	0.00869	0.8	98.8	98.2	1,431.59	2.29
1490–01L	•4.5	0.91	0.004	0.009	1.4	127.496	0.01333	1.2	100	98	1,427.55	1.72
Integ. Age=											1,407.00	6.00
(•) Plateau Age =								47.5			1,431.00	6.00

Sample ID/Run ID#	Power (W)	Ca/K	Cl/K	$^{36}Ar/^{39}Ar$	$\%^{36}Ar(Ca)$	$^{40}Ar^*/^{39}Ar$	^{39}Ar (Mol-14)	$\%^{39}Ar$	Cum. $\%^{39}Ar$	$\%^{40}Ar^*$	Age (Ma)	± 2σ
KSH03B-4, Run ID# 1649-01 (J = 0.01063 ± 0.000012):												
1649–01A	1.4	0.71	–0.023	0.773	0	63.963	0.00163	0.3	0.3	21.9	935.87	18.63
1649–01B	1.5	0.01	0.026	0.046	0	29.719	0.01930	3.4	3.7	68.6	495.28	1.84
1649–01C	1.6	0.04	0.037	0.088	0	108.713	0.03274	5.7	9.4	80.7	1,385.67	2.08
1649–01D	1.7	0.01	0.038	0.010	0	120.931	0.04035	7.1	16.5	97.6	1,491.22	1.71
1649–01E	1.8	0.01	0.039	0.004	0.1	128.042	0.05030	8.8	25.3	99.2	1,549.92	1.58
1649–01F	1.9	0.02	0.042	0.001	0.2	134.568	0.04979	8.7	34	99.7	1,602.17	1.58
1649–01G	•2.0	0.03	0.041	0.001	0.4	136.373	0.04531	7.9	41.9	99.8	1,616.35	1.72
1649–01H	•2.2	0.00	0.043	0.002	0	136.986	0.09693	17	58.9	99.6	1,621.14	1.25
1649–01I	•2.5	0.04	0.046	0.002	0.4	137.747	0.10428	18.3	77.1	99.6	1,627.08	1.30
1649–01J	•3.0	0.67	0.044	0.001	8.1	135.640	0.07779	13.6	90.7	99.8	1,610.60	1.41
1649–01K	•4.0	0.61	0.044	0.000	18.6	135.986	0.05296	9.3	100	99.9	1,613.32	1.47
Integ. Age=											1,559.00	3.00
(•) Plateau Age =								66			1,618.00	7.00
KSH03B–4. Run ID# 1649–02 (J = 0.01063 ± 0.000012):												
1649–02A	1.5	0.13	0.038	0.076	0	58.937	0.02366	5.3	5.3	72.5	877.56	2.48
1649–02B	1.7	0.04	0.044	0.013	0	123.563	0.08248	18.5	23.8	96.9	1,513.17	1.66
1649–02C	1.8	0.02	0.043	0.002	0.1	132.629	0.05645	12.7	36.5	99.6	1,586.80	1.76
1649–02D	1.9	0.00	0.044	0.001	0	135.781	0.05198	11.7	48.1	99.8	1,611.71	1.42
1649–02E	•2.0	0.03	0.047	0.001	0.6	136.990	0.04849	10.9	59	99.8	1,621.17	1.55
1649–02F	•2.2	0.00	0.048	0.002	0	136.895	0.09958	22.3	81.3	99.7	1,620.43	1.20
1649–02G	•2.5	0.32	0.045	0.000	13.4	137.088	0.04015	9	90.3	99.9	1,621.94	2.92
1649–02H	3	0.39	0.042	0.000	57.6	135.898	0.02367	5.3	95.6	100	1,612.63	2.63
1649–02I	4.2	0.20	0.038	0.003	0.8	134.646	0.01941	4.4	100	99.3	1,602.78	2.48
Integ. Age=											1,562.00	3.00
(•) Plateau Age =								42.2			1,621.00	3.00
KSH03A–127. Run ID# 1653–01 (J = 0.01063 ± 0.000012):												
1653–01A	1.4	7.59	0.126	0.050	2.1	32.921	0.00068	1	1	69.4	541.35	23.41
1653–01B	1.5	0.85	0.076	0.029	0.4	26.238	0.00944	14.1	15.1	75.6	443.82	2.63
1653–01C	1.6	0.21	0.046	0.022	0.1	61.277	0.01374	20.5	35.5	90.5	904.94	2.16
1653–01D	1.7	0.38	0.056	0.002	2.6	90.053	0.01136	16.9	52.5	99.4	1,211.53	4.10
1653–01E	1.8	0.29	0.087	0.003	1.3	135.947	0.01128	16.8	69.3	99.3	1,613.01	3.21
1653–01F	1.9	0.29	0.090	0.005	0.9	167.025	0.00537	8	77.3	99.2	1,841.64	4.58
1653–01G	2	1.43	0.088	0.006	3.5	178.386	0.00347	5.2	82.4	99.1	1,918.48	5.54
1653–01H	2.1	1.63	0.137	0.001	39.4	185.955	0.00480	7.1	89.6	99.9	1,967.92	5.48
1653–01I	2.2	2.00	0.146	0.009	3.2	201.191	0.00412	6.1	95.7	98.8	2,063.50	6.01
1653–01J	2.5	6.90	0.096	0.000	278.5	215.739	0.00166	2.5	98.2	100.1	2,150.27	11.68
1653–01K	4	13.20	0.080	0.008	24.1	211.677	0.00122	1.8	100	99.2	2,126.45	16.34
Integ. Age=											1,415.00	4.00

Sample ID/Run ID#	Power (W)	Ca/K	Cl/K	$^{36}Ar/^{39}Ar$	$\%^{36}Ar(Ca)$	$^{40}Ar^*/^{39}Ar$	^{39}Ar (Mol-14)	$\%^{39}Ar$	Cum. $\%^{39}Ar$	$\%^{40}Ar^*$	Age (Ma)	± 2σ
KSH03A–300. Run ID# 1652–01 (J = 0.01063 ± 0.000012):												
1652–01A	1.4	5.59	0.220	0.043	1.8	47.327	0.00031	1.2	1.2	79.3	735.20	52.54
1652–01B	1.5	7.39	0.107	0.056	1.8	16.327	0.00076	2.9	4.1	50.1	288.71	25.81
1652–01C	1.6	7.36	0.103	0.025	4	28.813	0.00166	6.3	10.4	80.1	482.03	10.44
1652–01D	1.7	2.35	0.086	0.019	1.7	59.190	0.00131	5	15.4	91.3	880.54	13.20
1652–01E	1.8	4.24	0.066	0.015	3.8	66.516	0.00110	4.2	19.6	93.8	964.78	16.26
1652–01F	1.9	15.52	0.041	0.014	15.6	65.687	0.00175	6.7	26.3	95	955.44	10.35
1652–01G	2	5.33	0.005	–0.001	–131.6	78.830	0.00266	10.2	36.4	100.5	1,098.07	6.98
1652–01H	2.1	2.97	0.009	0.001	29.8	83.731	0.00223	8.5	45	99.7	1,148.50	8.51
1652–01I	2.2	13.19	–0.003	0.001	158.3	81.795	0.00245	9.3	54.3	100.2	1,128.74	7.55
1652–01J	•2.5	4.20	0.024	0.005	10.6	63.982	0.00493	18.8	73.1	97.8	936.08	4.01
1652–01K	•3.0	14.04	0.036	0.005	38.7	62.601	0.00341	13.1	86.2	98.6	920.25	5.30
1652–01L	•4.2	11.30	0.024	0.005	31.5	62.776	0.00361	13.8	100	98.4	922.26	5.44
Integ. Age=											944.00	5.00
(•) Plateau Age =								45.7			928.00	6.00
KSH03A–1000. Run ID# 1645–01 (J = 0.01063 ± 0.000012):												
1645–01A	1.4	0.00	0.037	0.084	0	104.834	0.02545	2.4	2.4	80.9	1,350.83	2.26
1645–01B	1.6	0.00	0.042	0.003	0	118.935	0.30373	28.3	30.7	99.4	1,474.39	1.19
1645–01C	•1.8	0.00	0.042	0.000	0.2	120.108	0.27039	25.2	55.9	99.9	1,484.30	1.23
1645–01D	•2.0	0.01	0.040	0.001	0.1	120.032	0.22763	21.2	77.1	99.9	1,483.66	1.11
1645–01E	•2.2	0.00	0.039	0.000	0	119.887	0.15323	14.3	91.4	99.9	1,482.44	1.15
1645–01F	•2.4	0.00	0.033	0.000	0.7	120.134	0.04971	4.6	96	100	1,484.52	2.58
1645–01G	•2.6	0.08	0.030	0.000	7.5	120.117	0.01930	1.8	97.8	100	1,484.38	3.06
1645–01H	•2.8	0.09	0.014	0.002	0.7	120.079	0.00953	0.9	98.7	99.6	1,484.06	5.22
1645–01I	•3.0	0.57	–0.007	0.000	19	121.197	0.00482	0.4	99.2	99.9	1,493.45	9.84
1645–01J	•3.4	0.05	0.016	0.003	0.2	119.634	0.00882	0.8	100	99.3	1,480.31	3.83
Integ. Age=											1,478.00	3.00
(•) Plateau Age =								69.3			1,484.00	3.00
KSH03A–1000. Run ID# 1645–02 (J = 0.01063 ± 0.000012):												
1645–02A	1.3	0.13	0.192	0.908	0	171.700	0.00034	0.1	0.1	39	1,873.66	81.49
1645–02B	1.4	0.02	0.018	0.080	0	105.278	0.00776	1.6	1.6	81.7	1,354.85	4.34
1645–02C	1.5	0.00	0.034	0.009	0	115.529	0.03544	7.1	8.7	97.7	1,445.31	1.72
1645–02D	1.6	0.03	0.035	0.001	0.3	118.007	0.08065	16.1	24.8	99.6	1,466.52	2.06
1645–02E	•1.7	0.03	0.037	0.000	0.9	119.151	0.07955	15.9	40.7	99.9	1,476.22	1.74
1645–02F	•1.8	0.01	0.038	0.000	0.3	119.418	0.07183	14.4	55.1	99.9	1,478.48	2.10
1645–02G	•1.9	0.00	0.033	0.000	0.7	119.313	0.03845	7.7	62.8	100	1,477.59	1.84
1645–02H	•2.0	0.01	0.029	0.002	0.1	119.717	0.03008	6	68.8	99.6	1,481.01	2.70
1645–02I	•2.1	0.00	0.033	0.001	0.1	119.290	0.03774	7.5	76.4	99.8	1,477.40	2.36
1645–02J	•2.2	0.00	0.034	0.000	0.6	119.689	0.04157	8.3	84.7	100	1,480.77	1.83
1645–02K	•2.4	0.03	0.033	0.002	0.3	119.515	0.03468	6.9	91.6	99.6	1,479.30	1.88
1645–02L	•2.7	0.24	0.030	0.004	0.9	119.641	0.01891	3.8	95.4	99.1	1,480.37	3.03
1645–02M	•3.2	0.26	0.016	0.003	1.3	119.100	0.01093	2.2	97.6	99.3	1,475.79	3.50
1645–02N	•4.5	0.05	0.016	0.001	0.9	119.429	0.01210	2.4	100	99.8	1,478.57	2.85
Integ. Age=											1,473.00	3.00
(•) Plateau Age =								75.2			1,479.00	3.00

5.2 (U-Th)/He ages

When apatite crystallizes, U and Th are incorporated into the crystal lattice. Both isotopes subsequently decay with emission of alpha particles (= ^{4}He nuclei). Helium is completely mobile in apatite down to a temperature of c 60–70°C /Farley 2000/, after which it starts to be retained in the crystal. However, helium diffusion continues at lower temperatures, though at progressively slower rates, until complete retention occurs below c 40°C. This temperature range is referred to as the *He*lium *P*artial *R*etention *Z*one (HePRZ) and is analogous to the *P*artial *A*nnealing *Z*one (PAZ) used in apatite fission-track thermochronology /Gallagher et al. 1998/. Due to its lower temperature sensitivity, the (U-Th)/He method has been used in interdisciplinary fields within geomorphology, landform evolution, structural geology and geodynamics.

The (U-Th)/He data that have been used to calculate the ages presented in this report are listed in Table 5-3. These include age determinations from several levels of KLX01, KLX02, KSH03A/B and the access tunnel to the ÄHRL. The means that are mentioned in the text below are weighted means that include the internal errors stated in Table 5-3 and assigned external errors.

KLX01

The (U-Th)/He ages from drill core samples of Ävrö granite (and fine-grained granite at 600 m borehole length) in KLX01 basically decrease from top to bottom and are consistent in most cases within the individual levels (Figure 5-23). There seems to be an offset between 200 m and 400 m. The two splits at the 5 m level yield two different ages: 230 ± 16 Ma and 284 ± 21, of which none can be excluded for good reasons; the two splits at the 200 m level yield identical ages of 226 ± 17 Ma; the 400 m level yields a mean age of 261 ± 14 Ma; the 600 m level yield two largely different ages of 248 ± 20 Ma and 373 ± 26 Ma, of which the oldest is excluded from further discussion. The 800 m level yields a mean age of 230 ± 12 Ma.

KLX02

The (U-Th)/He ages from drill core samples of Ävrö granite, fine-grained dioritoid and fine-grained diorite-gabbro in KLX02 also decrease from top to bottom with a kink in the slope at c 1,400 m (Figure 5-24). The surface level yield two different ages: 273 ± 20 Ma and 313 ± 24 Ma, the youngest of which is interpreted to be closer to the true age. At 200 m the mean age of three analysis is 266 ± 11 Ma. The 400 m level yields two reproducing ages with a mean of 260 ± 27 Ma but also have an outlying age of 192 ± 12 Ma, which is disregarded in further discussion. The ages at the 600 m level are very close to reproducing and give a mean age of 227 ± 44 Ma. The 800 m level yields a mean age of 232 ± 77 Ma. At 1,000 m a mean of three analyses is 227 ± 27 Ma, a fourth analysis resulted in a too old age of 314 Ma and is excluded from further discussion. At 1,200 m the mean age is 206 ± 50 Ma and at 1,400 m there is only one analysis giving an age of 198 ± 16 Ma. At 1,600 m the mean age is 154 ± 39 Ma and at the lowermost level, 1,700 m, the mean age is 131 ± 35 Ma.

KSH03A/B

The (U-Th)/He ages from drill core samples of quartz monzodiorite and Ävrö granite in KSH03A/B decrease from top to bottom, here with an apparent offset at c 200 m (Figure 5-25). The mean age at 4 m is 229 ± 10 Ma; at 127 m: 205 ± 19 Ma; at 300 m: 245 ± 16 Ma; at 520 m: 234 ± 12 Ma; at 740 m: 241 ± 37 and at 1,000 m: 216 ± 26 Ma.

Table 5-3. (U-Th)/He data.

Sample ID	Sample split	Depth (m)	^{238}U (no of atoms or ppm)	^{235}U (no of atoms or ppm)	^{232}Th (no of atoms or ppm)	He (no of atoms or cm^3/g)	F_t[a]	Corr. Age[b] (Ma)	Error (± 1σ)
KLX01	p1	5	1.04E+11	7.55E+08	1.51E+11	2.40E+10	0.578	230	16
KLX01	p2	5	2.34E+11	1.70E+09	2.93E+11	7.02E+10	0.626	284	21
KLX01	p1	200	45.09	0.33	76.60	1.41E–03	0.813	226	17
KLX01	p2	200	19.74	0.14	33.98	5.93E–04	0.780	226	17
KLX01	p1	400	28.19	0.20	48.24	1.03E–03	0.814	264	21
KLX01	p2	400	37.45	0.27	50.04	1.20E–03	0.774	259	20
KLX01	p1	600	50.93	0.37	51.77	1.52E–03	0.798	248	20
KLX01	p2	600	35.71	0.26	42.50	1.41E–03	0.678	373	26
KLX01	p1	800	33.57	0.24	49.98	1.02E–03	0.788	235	18
KLX01	p2	800	52.60	0.38	87.07	1.55E–03	0.774	225	17
PSM000026	p1	0	3.07E+11	2.23E+09	3.32E+11	8.97E+10	0.654	273	20
PSM000026	p2	0	2.75E+11	1.99E+09	3.13E+11	9.61E+10	0.676	313	24
KLX02	p1	200	11.91	0.09	20.46	4.31E–04	0.815	260	20
KLX02	p2	200	24.26	0.18	45.24	8.54E–04	0.763	264	20
KLX02	p3	200	6.11	0.04	10.98	1.93E–04	0.672	272	18
KLX02	p1	400	21.32	0.15	50.30	7.52E–04	0.746	250	17
KLX02	p2	400	11.41	0.08	54.43	3.73E–04	0.660	192	12
KLX02	p3	400	23.73	0.17	71.20	8.26E–04	0.626	268	16
KLX02	p1	600	45.50	0.33	66.50	1.10E–03	0.693	213	15
KLX02	p2	600	42.39	0.31	71.02	1.26E–03	0.723	242	16
KLX02	p1	800	37.13	0.27	79.07	1.17E–03	0.725	238	16
KLX02	p2	800	59.78	0.43	96.49	1.53E–03	0.673	226	15
KLX02	p1	1,000	26.15	0.19	44.59	1.00E–03	0.719	314	15
KLX02	p2	1,000	49.60	0.36	80.24	1.26E–03	0.682	222	15
KLX02	p3	1,000	36.84	0.27	46.29	9.01E–04	0.687	226	16
KLX02	p4	1,000	10.27	0.07	11.07	2.24E–04	0.615	233	15
KLX02	p1	1,200	14.34	0.10	27.38	3.73E–04	0.778	190	14
KLX02	p2	1,200	13.18	0.10	28.03	3.61E–04	0.674	223	14
KLX02	p1	1,400	3.32	0.02	6.33	7.95E–05	0.686	198	16
KLX02	p1	1,600	18.42	0.13	34.42	3.23E–04	0.708	141	10
KLX02	p2	1,600	22.23	0.16	61.13	4.87E–04	0.654	167	10
KLX02	p2	1,700	18.41	0.13	40.94	2.91E–04	0.714	120	8
KLX02	p3	1,700	5.05	0.04	10.54	8.54E–05	0.653	143	11
Tunnel	p1	0	13.89	0.10	20.45	4.32E–04	0.801	237	18
Tunnel	p2	0	20.73	0.15	26.87	6.18E–04	0.731	257	19
Tunnel	p1	100	20.38	0.15	36.19	6.54E–04	0.752	247	18
Tunnel	p2	100	29.88	0.22	34.26	9.08E–04	0.737	267	21
Tunnel	p3	100	14.72	0.11	21.28	5.55E–04	0.686	338	23
Tunnel	p1	300	5.94	0.04	12.24	1.83E–04	0.708	241	16
Tunnel	p2	300	14.33	0.10	23.58	4.43E–04	0.635	289	18
Tunnel	p3	300	9.93	0.07	23.13	2.75E–04	0.581	253	14
Tunnel	p1	400	12.57	0.09	19.02	7.76E–04	0.770	486	37
Tunnel	p2	400	12.15	0.09	25.42	4.51E–04	0.708	289	20
Tunnel	p1	500	11.91	0.09	31.61	4.53E–04	0.700	275	20
Tunnel	p2	500	12.01	0.09	39.67	4.32E–04	0.785	212	15
KSH03B	p1	4	4.48E+11	3.25E+09	6.16E+11	1.46E+11	0.719	263	18
KSH03B	p2	4	2.09E+11	1.51E+09	3.06E+11	6.73E+10	0.808	228	16
KSH03B	p3	4	3.41E+11	2.47E+09	8.05E+11	1.27E+11	0.810	227	21
KSH03B	p4	4	1.89E+12	1.37E+10	2.14E+12	6.28E+11	0.872	230	16
KSH03A	p1	127	1.75E+11	1.27E+09	1.54E+11	3.73E+10	0.617	220	17
KSH03A	p2	127	2.49E+11	1.81E+09	2.35E+11	5.65E+10	0.640	223	16
KSH03A	p3	127	3.41E+11	2.48E+09	3.27E+11	7.33E+10	0.714	189	13
KSH03A	p4	127	7.92E+11	5.74E+09	6.17E+11	1.81E+11	0.779	191	13
KSH03A	p1	300	1.96E+11	1.42E+09	3.43E+11	6.21E+10	0.692	250	18
KSH03A	p2	300	2.61E+11	1.90E+09	4.21E+11	8.45E+10	0.658	274	26
KSH03A	p3	300	6.74E+11	4.89E+09	1.11E+12	2.15E+11	0.757	233	16
KSH03A	p4	300	4.18E+11	3.03E+09	6.59E+11	1.33E+11	0.754	236	16
KSH03A	p1	520	1.33E+11	9.68E+08	2.05E+11	3.74E+10	0.669	237	20
KSH03A	p2	520	1.60E+11	1.16E+09	2.38E+11	4.43E+10	0.682	231	17
KSH03A	p1	740	8.71E+10	6.31E+08	2.66E+11	2.78E+10	0.564	255	19
KSH03A	p2	740	6.68E+10	4.84E+08	1.47E+11	1.83E+10	0.601	232	28
KSH03A	p3	740	9.90E+10	7.18E+08	2.68E+11	2.95E+10	0.611	231	21
KSH03A	p1	1,000	1.26E+12	9.14E+09	1.24E+12	4.31E+11	0.821	259	18
KSH03A	p2	1,000	8.58E+11	6.23E+09	1.10E+12	2.36E+11	0.729	222	18
KSH03A	p3	1,000	6.45E+11	4.68E+09	8.76E+11	1.89E+11	0.764	224	15
KSH03A	p4	1,000	6.48E+11	4.70E+09	6.07E+11	1.65E+11	0.778	206	14

[a] F_t= alpha-ejection correction factor.

[b] Raw age corrected with respect to F_t.

[c] Depth in tunnel is approximately elevation.

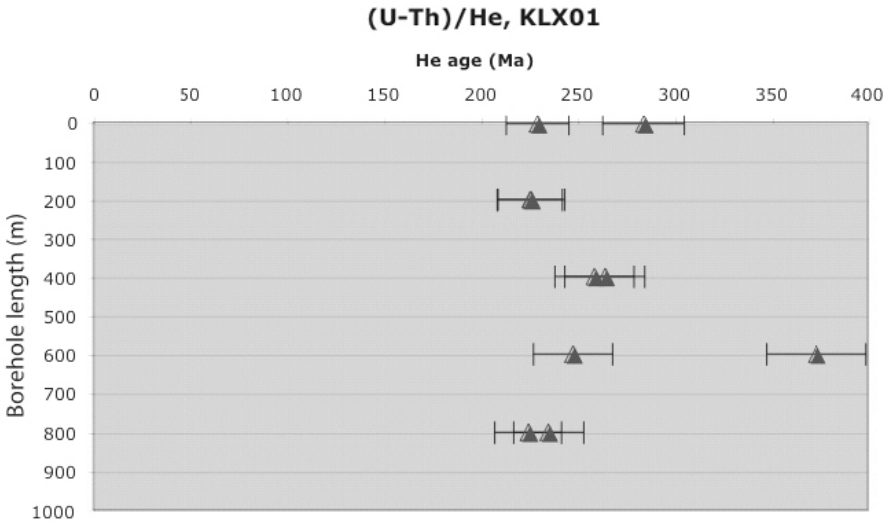

Figure 5-23. *(U-Th)/He age vs borehole length profiles for borehole KLX01.*

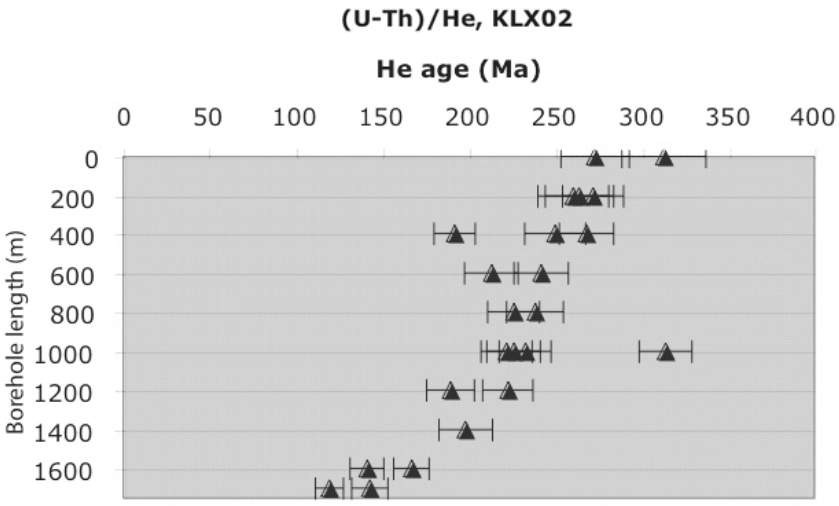

Figure 5-24. *(U-Th)/He age vs borehole length profiles borehole for KLX02.*

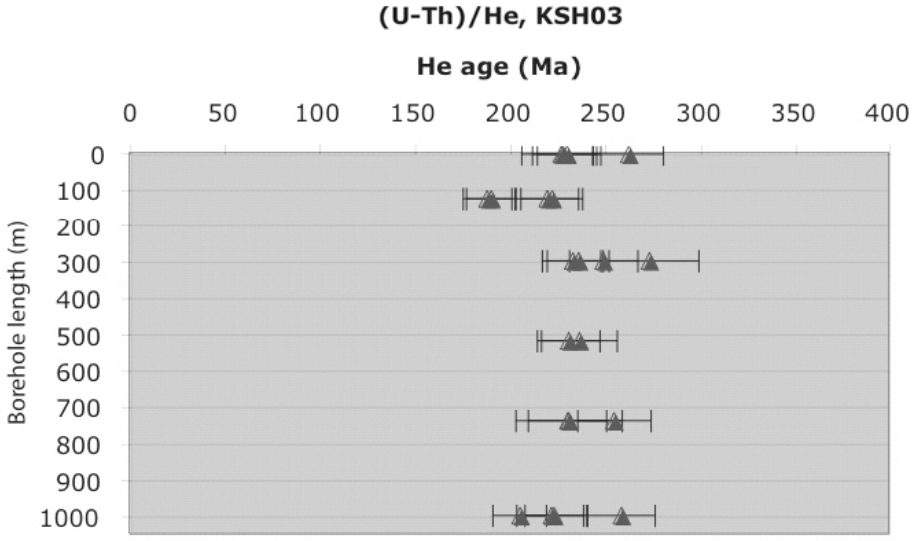

Figure 5-25. *(U-Th)/He age vs borehole length profiles for borehole KSH03.*

Access tunnel to ÄHRL

The (U-Th)/He ages of samples from the access tunnel to ÄHRL displays a slightly more spread at each individual level than the ages from the drill core samples (Figure 5-26). Within errors the ages are more or less consistent from top to bottom. At surface level the mean age is 247 ± 31 Ma. At 100 m depth the mean age of two splits is 256 ± 30 Ma, a third analysis yielded a too old age of 338 ± 23 Ma. At 300 m the mean age is 261 ± 31 Ma. The ages at 400 m are not reproducible, one age is 486 ± 37 Ma and the other 289 ± 20 Ma. The oldest age falls well out of range from the other ages in the tunnel and is therefore excluded from further discussion. The reason for the old age may be an undetected inclusion. The 500 m level yields a mean of 243 ± 96 Ma. The reason for the high error is that the two ages do not reproduce within errors but are both within the general age-trend of the tunnel.

Discussion

Presently, there is an ongoing discussion in the scientific community regarding the interpretation of (U-Th)/He ages from old and slowly cooled geological terrains /cf Hendriks and Redfield 2005, Shuster et al. 2006/. In the following sections the (U-Th)/He ages are interpreted in the classical way, i.e. α-ejection corrected ages represent cooling below 70°C.

The (U-Th)/He ages from the drill cores from KLX01, KLX02 and KSH03A/B as well as the (U-Th)/He ages from the access tunnel to ÄHRL are in good agreement. Although some surface ages vary a bit they all range between c 225 and c 285 Ma. There are indications that the ages thereafter decrease with increasing depth, down to c 200 Ma at 1,000 m borehole length. However, some ages seem to be off-set in regard to levels immediately above/below the level in question. These off-sets may indicate zones of movement.

The (U-Th)/He ages from the drill cores show that the rocks, down to c 1,000 m, in the Oskarshamn area has not been heated above 70°C since c 200 My. The ages also indicate that there has been some brittle movement sometime after 200 My. In some cases, where the ages show a trend with decreasing ages with depth, it is possible to use the ages to calculate an exhumation rate.

The ages presented here are younger than AFT ages presented in /Larson et al. 1999/ for three samples taken from borehole KLX02 at depths of 3,994 and 1,694 m which yielded ages of 340 ± 8, 264 ± 8 and 206 ± 6 Ma, respectively. This is to be expected due to the lower closure temperature of the (U-Th)/He system in apatite. A detailed comparison of the results is discussed in /Söderlund et al. 2005/.

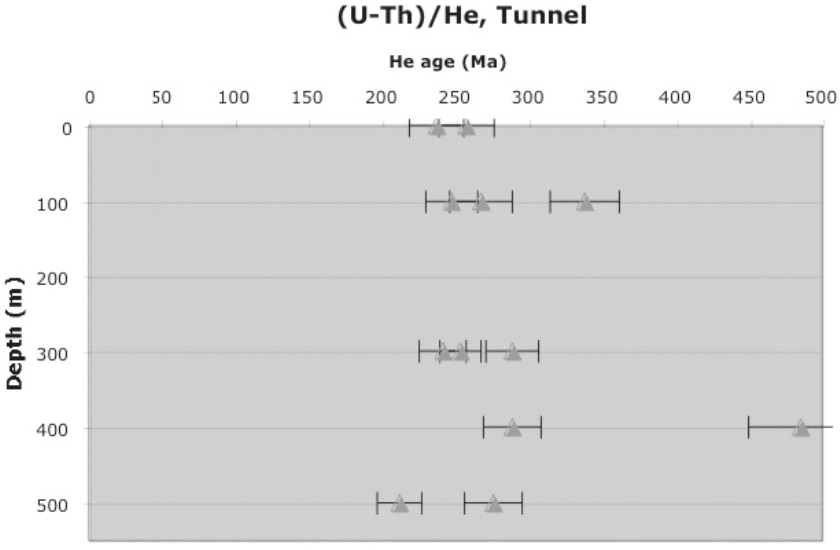

Figure 5-26. *(U-Th)/He age vs depth profiles for access tunnel to ÄHRL.*

KLX01

Ages from drill core KLX01 are off-set with regard to the 200 m level and the 400 m level (Figure 5-27). The off-set may be an indication that the rocks presently below 300 m have been down-faulted to their present location sometime after the (U-Th)/He ages where established in the rock, i.e. after c 250 Ma. However, no deformation zone has been detected at the level in question during the geological single-hole interpretation /Carlsten et al. 2004/.

The ages from the 400 m level and downward yield a trend from which an exhumation rate can be calculated. The exhumation rate is c 13 m/My, which is in perfect agreement with the exhumation rate calculated from KLX02 see below and /Söderlund et al. 2005/.

KLX02

KLX02 is the deepest borehole, reaching down to 1,700 m. The (U-Th)/He ages decrease linearly down to c 1,400 m where the slope changes direction, which indicate that an abrupt change in cooling and/or uplift rate occurred see also /Söderlund et al. 2005/ (Figure 5-28). Calculations and modelling of the (U-Th)/He ages in /Söderlund et al. 2005/ showed that the change probably occurred as late as c 100 My ago. The exhumation rate registered from the upper part of the drill core is in perfect agreement with the exhumation rate calculated from KLX01, i.e. 13 m/Ma. The ages from the lower part of KLX02 give an exhumation rate of c 4 m/Ma. Far-field effects of the gravitational collapse of the Caledonides possibly caused prolonged exhumation of the rim of the foreland basin. The data set from KLX02 indicate that this exhumation finally stopped at c 100 Ma see /Söderlund et al. 2005/ for further explanation. Since KLX02 is the only borehole that is drilled far below 1,000 m this is the drill core where such a detailed history can be achieved.

Geological single hole interpretation /Hultgren et al. 2004/ indicate a deformation zone at 770–960 m but the (U-Th)/He ages do not show any off-set around this level why the zone has not had any movement along it during the last 250 My, but has to have an older history.

KSH03A/B

The age profile of KSH03A/B (Figure 5-29) resembles the ages from KLX01. Even in KSH03 there may be an off-set, but between 130 and 300 m borehole length. Interestingly, earlier studies show a large deformation zone between 160 and 275 m borehole length /Hultgren et al. 2004/. Movement along this zone may have occurred sometime after 250 Ma, moving the rocks to their current position. The zone, however, can have developed during an earlier active stage indicated by large differences in Ar-ages at top and bottom of the drill core as well as incomplete reset of Ar ages from samples in close relation to the zone (this report).

Access tunnel to ÄHRL

The tunnel does not reach the same depth as the drill cores and, thus, the ages seem to decrease less with depth at first glance. However, at 500 m depth the age is c 240 Ma, which is in perfect agreement with all three drill cores at corresponding level. Regarding the ages there is no indication of any significant off-set in the tunnel.

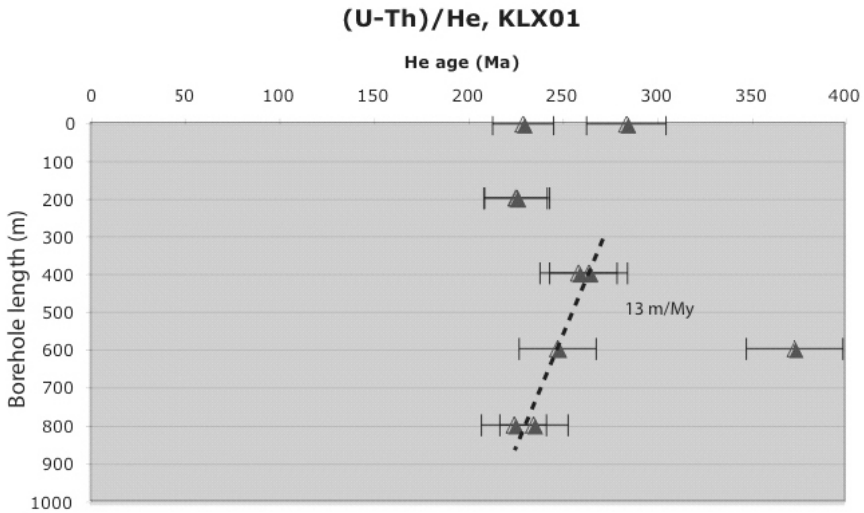

Figure 5-27. *(U-Th)/He age vs borehole length profiles for borehole KLX01.*

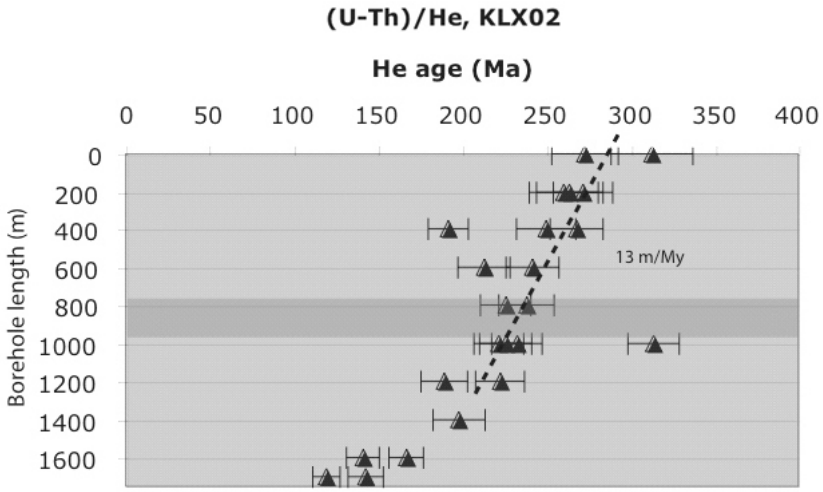

Figure 5-28. *(U-Th)/He age vs borehole length profiles for borehole KLX02. The red band marks an identified deformation zone from the geological single-hole interpretation.*

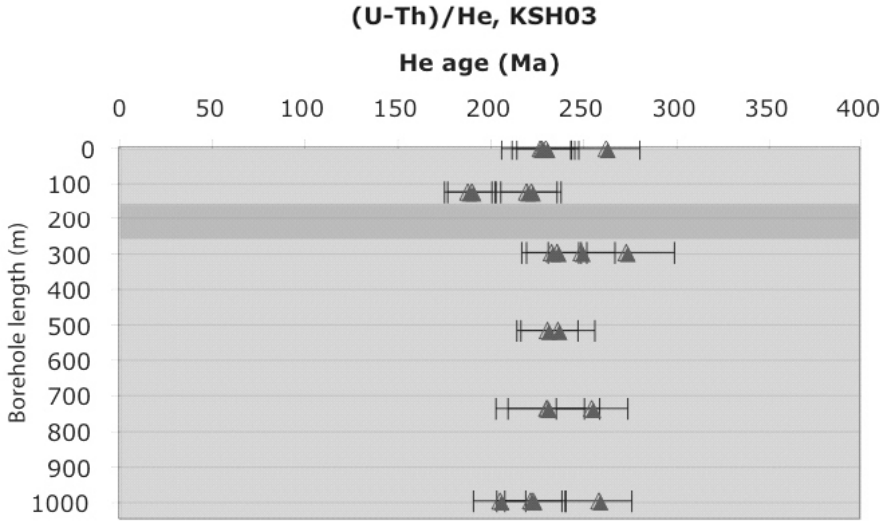

Figure 5-29. *(U-Th)/He age vs borehole length profiles for borehole KSH03. The red band marks an identified deformation zone from the geological single-hole interpretation.*

6 References

Carlsten S, Hultgren P, Mattsson H, Stanfors R, Wahlgren C-H, 2004. Oskarshamn site investigation.Geological single-hole interpretation of KAV04A, KAV04B and KLX01. SKB P-04-308, Svensk Kärnbränslehantering AB.

Dalrymple G B, Lanphere M A, 1971. $^{40}Ar/^{39}Ar$ technique of K-Ar dating: a comparison with the conventional technique. Earth Planet. Sci, Lett., 12, 300–308.

Drake H, Page L, Tullborg E L, 2006. Oskarshamn site investigation. $^{40}Ar/^{39}Ar$ dating of fracture minerals. SKB P-07-27, Svensk Kärnbränslehantering AB.

Dörr W, Belka Z, Marheine D, Schastok J, Valverde-Vaquero P, Wiszniewska J, 2002. U-Pb and Ar-Ar geochronology of anorogenic granite magmatism of the Mazury complex, NE Poland. Precambrian-Research.119 (1-4), 101–120.

Farley K A, 2000. Helium diffusion from apatite: general behavior as illustrated by Durango flourapatite. Journal of Geophysical Research 105, 2903–2914.

Gallagher K, Brown R, Christopher J, 1998. Fission-track analysis and its applications to geological problems. Annual Revue of Earth and Planetary Science 26, 519–572.

Hendriks B W H, Redfield T F, 2005. Apatite fission track and (U-Th)/He data from Fennoscandia: an example of underestimation of fission track annealing in apatite. Earth and Planetary Science Letters 236: 443–458.

Hultgren P, Stanfors R, Wahlgren C-H, Carlsten S, Mattsson H, 2004. Oskarshamn site investigation. Geological single-hole interpretation of KSH03A, KSH03B, KLX02, HAV09 and HAV10. SKB P-04-231, Svensk Kärnbränslehantering AB.

Larson S Å, Tullborg E L, Cederbom C E, 1999. Sveconorwegion and Caledonian foreland basins in the Baltic Shield revealed by fission-track thermochronology. Terra Nova 11, 210–215.

Lundberg E, Sjöström H, 2006. Oskarshamn site investigation. Kinematic analysis of ductile and brittle/ductile shear zones in Simpevarp and Laxemar subarea. SKB P-06-118, Svensk Kärnbränslehantering AB.

McDowell F W, McIntosh W C, Farley K A, 2005. A precise $^{40}Ar/^{39}Ar$ reference age for the Durango apatite (U-Th)/He and fission track dating standard. Chemical Geology 25; 214(3–4): 249–263.

Page L, Hermansson T, Söderlund P, Stephens M B, 2006. Forsmark site investigation: $^{40}Ar/^{39}Ar$ and (U-Th)/He geochronology Phase II. Reviewed report SKB P-06-211, Svensk Kärnbränslehantering AB.

Renne P R, Swisher C C, Deino A L, Karner D B, Owena T L, DePaolo D J, 1998. Intercalibration of standards, absolute ages and uncertainties in $^{40}Ar/^{39}Ar$ dating. Chem. Geol., 145: 117–152.

Shuster L, Feowers R M, Farley K A, 2006. The influence of natural radiation damage on helium diffusion kinetics in apatite. Earth and Planetary Science Letters 249: 148–161.

SKB, 2006. Preliminary site description. Laxemar subarea – version 1.2. SKB R-06-10, Svensk Kärnbränslehantering AB.

Söderlund P, Juez-Larré J, Page L, Dunai T, 2005. Extending the time range of apatite (U-Th)/He thermochronometry in slowly cooled terranes: Palaezoic to Cenozoic exhumation history of southeast Sweden. Earth and Planetary Science Letters 239: 266–275.

Wahlgren C-H, Hermanson J, Curtis P, Forsberg O, Triumf C-A, Drake H, Tullborg E L, 2006. Geological description of rock domains and deformation zones in the Simpevarp and Laxemar subareas. Preliminary site description Laxemar subare – version 1.2. SKB R-05-69, Svensk Kärnbränslehantering AB.